# CENTER FOR TRANSPORTATION INFRASTRUCTURE AND SAFETY

## Cyclic Behavior of Self-Consolidated Concrete

by

Mohamed ElGawady, PhD
Associate Professor
Department of Civil, Architectural & Environmental Engineering
Missouri University of Science and Technology

Aly Said Ph.D., P.E.
Associate Professor
Department of Civil and Environmental Engineering and Construction
Director, Center for Materials and Structures
University of Nevada Las Vegas

Pramen Shrestha Ph.D., P.E.
Associate Professor
Department of Civil and Environmental Engineering and Construction
University of Nevada Las Vegas

and

Kojo Nkuako M.S.
Graduate Student
Department of Civil and Environmental Engineering and Construction
University of Nevada Las Vegas

**NUTC
R326**

**A National University Transportation Center
at Missouri University of Science and Technology**

**Technical Report Documentation Page**

| 1. Report No.<br><br>NUTC R326 | 2. Government Accession No. | 3. Recipient's Catalog No. | |
|---|---|---|---|
| 4. Title and Subtitle<br>Cyclic Behavior of Self-Consolidated Concrete | | 5. Report Date<br><br>August 2014 | |
| | | 6. Performing Organization Code | |
| 7. Author/s<br><br>Mohamed ElGawady, Aly Said, Pramen Shrestha, and Kojo Nkuako | | 8. Performing Organization Report No.<br><br>  Project #00041156 | |
| 9. Performing Organization Name and Address<br><br>Center for Transportation Infrastructure and Safety/NUTC program<br>Missouri University of Science and Technology<br>220 Engineering Research Lab<br>Rolla, MO 65409 | | 10. Work Unit No. (TRAIS) | |
| | | 11. Contract or Grant No.<br><br>DTRT06-G-0014 | |
| 12. Sponsoring Organization Name and Address<br><br>U.S. Department of Transportation<br>Research and Innovative Technology Administration<br>1200 New Jersey Avenue, SE<br>Washington, DC 20590 | | 13. Type of Report and Period Covered<br><br>Final | |
| | | 14. Sponsoring Agency Code | |
| 15. Supplementary Notes | | | |

16. Abstract
This reports highlights on the production of Self-Consolidating concrete using local materials from Las Vegas, Nevada. 4 SCC mixtures were worked on with 2 different levels of FA replacement and the inclusion of superplasticizers, ADVA 195 and V-MAR 3. The fresh properties tested of these mixtures are the flowability, passing ability and the stability. The mechanical properties were also ascertained and these comprised of the compressive strength, splitting tensile strength and the modulus of elasticity. The durability of the specimens produced from the mixtures was tested against chloride ion resistance, sulfate resistance and salt scaling. The effect of the concrete constituents on the results obtained from fresh and hardened properties are also discussed. Moreover, this report investigates the difference in the behavior of SCC and conventional concrete encased in fiber reinforced polymer tubes. The effect of fiber orientation on both strength and ductility of FRP confined concrete is discussed. Axial compression tests were performed under monotonic and cyclic conditions to determine the stress strain relationship of a self-consolidating concrete filled fiber tube with ±45° fibers. The test results obtained from the compression tests are presented and examined.

| 17. Key Words<br><br>Seismic-rubberized concrete- damping- highway sound barrier walls | 18. Distribution Statement<br><br>No restrictions. This document is available to the public through the National Technical Information Service, Springfield, Virginia 22161. | | |
|---|---|---|---|
| 19. Security Classification (of this report)<br><br>unclassified | 20. Security Classification (of this page)<br><br>unclassified | 21. No. Of Pages<br><br>87 | 22. Price |

Form DOT F 1700.7 (8-72)

# SUMMARY

This reports highlights on the production of Self-Consolidating concrete using local materials from Las Vegas, Nevada. 4 SCC mixtures were worked on with 2 different levels of FA replacement and the inclusion of superplasticizers, ADVA 195 and V-MAR 3. The fresh properties tested of these mixtures are the flowability, passing ability and the stability. The mechanical properties were also ascertained and these comprised of the compressive strength, splitting tensile strength and the modulus of elasticity. The durability of the specimens produced from the mixtures was tested against chloride ion resistance, sulfate resistance and salt scaling. The effect of the concrete constituents on the results obtained from fresh and hardened properties are also discussed. Moreover, this report investigates the difference in the behavior of SCC and conventional concrete encased in fiber reinforced polymer tubes. The effect of fiber orientation on both strength and ductility of FRP confined concrete is discussed. Axial compression tests were performed under monotonic and cyclic conditions to determine the stress strain relationship of a self-consolidating concrete filled fiber tube with ±45° fibers. The test results obtained from the compression tests are presented and examined.

# TABLE OF CONTENT

# LIST OF TABLES

# LIST OF FIGURES

# INTRODUCTION

Self-consolidating concrete (SCC) is a specially engineered concrete which is highly stable and less prone to segregation, capable of flowing under its own weight through highly congested spaces and does not require any external and/or mechanical vibration[1, 2,3,4,5]. SCC has gained a lot of popularity in recent years because of some desired attributes it embodies, and this has led to myriads of research been done to ascertain it practicality. Due to the extensive specification and use of SCC by engineering professionals in North America, SCC has been tagged as an Industry Critical Technology by the Strategic Development Council in order to push for 15% of all ready mix to be SCC by the year 2015 [3].

SCC usage in the construction industry provides quite a number advantages and benefits to the clients, consultants and the contractors. Even though it can be debated that the short term cost of producing SCC is higher than that of normal vibrated concrete (NVC), the overall cuts in the cost of operation and construction is undeniably less. There is a significant reduction in man-hours because of the elimination of the need for personnel to vibrate concrete during placement. Furthermore, there a significant reduction in noise pollution enabling the neighbors of the construction project to enjoy low levels of disturbances. Structurally, it ensures the flexibility of the role of designers with regards to producing detailing of their designs. They have the liberty of producing designs in which highly congested reinforcement is required per the expected demand of the structure. Due to the fluidity, self-consolidating and stability of the concrete mass, little restraints and work is required to ensure concrete placement and realization of the concrete structure.

The difference in the composition and properties of local materials and the different admixtures producers are warranting factors to determine the properties of the SCC designed for use in a particular project location. This research seeks to investigate the effect of the local materials and the admixtures, ADVA 195 and V-MAR 3, on the properties of SCC to be used in Nevada Department of Transportation (NDOT) projects like the bridge construction in Mesquite. All specimen fabrication and testing conducted at the laboratory were conducted under complete compliance with the American Standards for Testing Materials (ASTM).

# LITERATURE REVIEW

## 2.1 Fresh Properties of SCC

In selecting SCC as a building material, one wishes to utilize the increased workability that SCC provides in comparison with conventional (vibrated) concrete. This workability can be divided into three main properties: (1) filling ability, (2) passing ability and (3) resistance to segregation. Filling ability describes the potential for fresh SCC to fill formwork and properly surround reinforcement within the form. Passing ability for SCC allows the fresh mixture to pass through reinforcement without becoming congested or being able to pass narrow portions of the formwork without aggregate accumulating and causing a blockage. Finally, resistance to segregation prevents suspended particles from settling within the fresh mix and causing a non-homogeneous condition within the fresh or hardened states [4, 5].

Rheology, the study of flow and deformation, must be considered and integrated with the workability properties [1, 6]. There are several available models applied when determining the rheological properties of SCC and involve the shear and yield stresses, plastic viscosity and shear strain of fresh mixture concrete [7]. A basic rheological model is the Bingham Fluid Model, which relates these properties as a straight-line function, including the abovementioned parameters. Recently, rheology has been compared to flow properties of fresh SCC in order to find correlations between the different parameters. Properties such as stability can be optimized when utilizing rheology properties. Furthermore, several tests such as the V-funnel can be used to quantify rheological parameters like viscosity. While correlations may exist, differences in testing apparatuses can cause different values using similar SCC mixtures. Interpreting the data that rheology tests provide and being able to apply it between various testing apparatuses becomes a challenge. Using standardized equipment between testing organizations would prove

useful, however, it is imperative to use one testing device throughout the duration of any laboratory testing.

Filling ability can be measured using the slump flow and $T_{20}$ ($T_{50}$) tests. These tests are described in detail in ASTM C1611, "Slump Flow of Self-Consolidating Concrete" and use similar equipment to ASTM C143, "Standard Test Method for Slump of Hydraulic-Cement Concrete", which is used to measure slump of conventional concrete [8-10]. Included within ASTM C1611 is the T-20 parameter which is the time taken for the slump flow disk to reach a diameter or 20 inches (50 centimeters). T20 has an expected time between two and seven seconds [8]. Filling ability may be increased using several methods such as higher fine content, reduced aggregate quantity, viscosity-modifying admixtures (VMA) and appropriate water/cement ratio [7]. Slump flow can also be controlled by monitoring water content and high-range water reducing admixtures. As well, determining the appropriate time to add admixtures to the fresh concrete mixture is vital. On-site adjustments to admixtures and water content should be made in order to obtain the desired slump flow for the project, as the properties of concrete mixture may have changed during transport or while waiting to be used at the job site. Careful monitoring of slump flow and in-line testing of the fresh concrete properties is required.

Passing ability is quantified using several tests including the V-funnel, L-box, U-box and J-ring tests (ASTM C1621 "Standard Test Method for Passing Ability of Self-Consolidating Concrete by J-Ring") [11]. Applications of these tests measure the ability of fresh concrete initially at rest to pass through congested reinforcement or through narrow openings where coarse aggregate may accumulate and cause a blockage. In comparison to conventional concrete, a much higher passing ability is expected due to increased workability associated with SCC. To

increase the passing ability of SCC, several techniques may be used; these include: low coarse

aggregate amount, reduced coarse aggregate size, use of a VMA and low water/cement ratio [7].

Resistance to segregation (also referred to as stability) is measured in several methods.

Such methods include the column segregation test, the penetration apparatus test and the visual

stability index (VSI) test (ASTM C1610, "Standard Test Method for Static Segregation of Self-

Consolidation Using Column Technique", ASTM C1712 "Standard Test Method for Rapid

Assessment of Resistance of Self-Consolidating Concrete Using Penetration Test", and ASTM

C1611 "Standard Test Method for Slump Flow of Self-Consolidating Concrete", respectively)

[8, 12, 13]. These tests measure the static stability of fresh SCC by allowing the mixture to

segregate under its own weight without mechanical vibration. Static stability is measured by

either performing a sieve analysis, measuring penetration within the fresh mixture or by visual

analysis. Dynamic stability refers to segregation resistance while the fresh SCC is being

transported or placed and analyzed using the passing ability tests. As with the other workability

properties, segregation resistance is increased by smaller coarse aggregate, low water/cement

ratio, and use of a VMA [7, 14]. These methods achieve segregation resistance by reducing the

segregation of solids and reducing the bleeding within the fresh mixture. Furthermore,

segregation can be minimized by increasing the cohesiveness of the mixture. This is done

through two methods: addition of fines to reduce the amount of free water within the mixture or

by using a VMA to increase the viscosity of the mixture. A combination of these two methods

may also be used when there are uncontrolled moisture conditions [7]. Ultimately, the

workability of SCC is increased by controlling a few parameters: amount of coarse and fine

aggregate, water/cement ratio, the use of a VMA and proper mixture design.

**2.2 Hardened SCC Properties**

For SCC to be a viable alternative, it must exhibit the same or nearly the same hardened characteristics as conventional concrete. Several key properties of cured concrete include compressive strength, modulus of elasticity, creep and durability.

A key aspect of SCC mixture design is reduction in water/cement ratio when compared to conventional concrete. Compressive strength of concrete mixtures is inversely proportional to the water/cement ratio, giving SCC a typically higher compressive strength. The mixture design of the SCC also has a significant effect on the compressive strength as a higher amount of fines is used, whether it is in the form of additional cement, fly ash, or other pozzolanic materials. The addition of fines increases the amount of cementitious material and therefore the compressive strength.

The modulus of elasticity (Young's Modulus) of concrete is affected directly by the amount of coarse aggregate and the modulus of that aggregate. Since SCC typically incorporates a lower amount of coarse aggregate, the modulus of elasticity may be lower than similar conventional concrete mixtures. As well, an increase of fines within the mixture may cause the same effect resulting in a reduction of the modulus of elasticity. Because of variation of SCC mixture design to conventional concrete mixture design, using standard equations to calculate the modulus using compressive strength may not accurately represent the actual modulus of elasticity for SCC.

Creep is the deformation of hardened concrete caused by stresses from various sources over time. SCC typically has a reduced water/cement ratio caused by superplasticizers and increased fine aggregate. As the concrete cures, water within the mixture becomes consumed at the core before fully hydrating, causing autogenous shrinkage. Drying shrinkage may also occur

when water trapped within the cement paste becomes lost to evaporation. External forces may be applied to concrete not yet fully cured, such as pre-stress and construction loads, and can cause additional deformation. The onset of creep in SCC comes early as low water cement ratios produce autogenous shrinkage.

Durability, as defined by ACI, "is determined by its ability to resist weathering action, chemical attack, abrasion, or any other process of deterioration [15]." Some of these processes include freeze-thaw cycles, alkali-aggregate reactions, reinforcement corrosion, and abrasion. If this is allowed to occur, weakening of concrete occurs in various forms and satisfactory concrete performance will diminish as these processes continue. Proper mixture design, admixture usage and understanding of these processes are pivotal in preventing long-term damage or extensive maintenance and repair of concrete.

## 2.3 Mixture Design for SCC

SCC differs from conventional concrete in its fresh state and must be designed specifically to obtain the desired properties (filling ability, passing ability, stability). These three properties can be developed using similar methods during mixture design. In general, SCC (as compared to conventional concrete) has a lower coarse aggregate content and size, a higher fine/paste content, a reduced water/cement ratio, and the addition of a VMA and/or superplasticizers. The quantities or proportions of each must be carefully calculated and tested to obtain job-specific requirements. There are three distinct types of SCC mixtures: (1) powder mixture, (2) VMA mixture or (3) a combination of the two. Powder mixtures involve higher amounts of cementitious materials, whereas VMA mixtures use admixtures to achieve the same effect. Combination mixtures utilize a blend of both mixture types.

While there are three types of SCC mixtures, the methodologies for designing these mixtures can vary greatly in approach in determining material amounts and proportions. The mixture design is dependent upon the use of the concrete member and the desired fresh properties. Proportions available within ACI 211.1 (Standard Practice for Selecting Proportions for Normal, Heavyweight and Mass Concrete) and ACI 301 (Specifications for Structural Concrete) may not be desirable for SCC as fresh concrete characteristics may not be achieved [16,17]. An example of this is maximum allowable aggregate size and the effect it has on passing ability. Larger aggregates may cause accumulation within formwork, while allowed in conventional mixture designs, may be detrimental to SCC mixtures.

Several sources reference the rational mixture design method proposed by Okamura and Ozawa. This procedure fixes the coarse and fine aggregate content, leaving only the water/cement ratio and amount of admixtures free to change. According to this design, coarse aggregate is 50% of the concrete solids and fine aggregate comprises 40% of the mortar. *PCI Interim Guidelines for SCC* uses an adaptation of Okamura and Ozawa's method. This adapted design begins with determining the target air content for the hardened concrete. From there, coarse aggregate, sand and mortar paste composition is determined. Afterwards, admixtures are added to the fresh mixture and water content is adjusted to fully utilize these admixtures. Finally, tests are completed on the mixture and adjustments are determined [18]. ACI 237, Self-Consolidating Concrete gives similar mixture design guidance, but replaces the desired air content with a desired slump flow requirement. This method is also referenced within "The European Guidelines for Self Compacting Concrete". The European Guideline mixture designs determine the appropriate amount of water needed for flow and stability [14].

Additional mixture design methodologies include the "Chinese Method" proposed by Su et al. This method determines the aggregate volume and then determines the mixture proportions of the binder. Aggregates are combined and loosely packed, leaving the voids within the aggregate structure needing to be filled by the binder. When compared to the method proposed by Okamura and Ozawa, the "Chinese Method" saves on cost by using a reduced amount of binder and by using an increased amount of sand. As well, the mixture design is typically easier to determine [19, 20]. Also, this method follows a standard particle size distribution for aggregate, the Andreasen and Andersen curve, whereas Okamura and Ozawa's method may not inherently follow such a distribution [20]. Regardless of which methodology is used to create the SCC mixture, nearly all reviewed literature suggests consultation of a professional SCC mixture designer to obtain the required, job-specific performance.

The tables below show examples of mixture designs from three different regions (Japan, Europe and the United States). For each region, a powder-type (mixture 1) used in a liquefied natural gas tank, a VMA-type (mixture 2) used in a caisson foundation and a combination type mixture design (mixture 3) used in structural concrete are shown. HRWR represents high-range water reducing admixtures and VMA represents viscosity-modifying admixtures [21].

Table 2.1 SCC Mixtures in Japan [22]

| Ingredient | Mixture 1 (powder) | Mixture 2 (VMA) | Mixture 3 (combination) |
|---|---|---|---|
| Water, kg | 175 | 165 | 175 |
| Portland Cement, kg | 530 | 220 | 298 |
| Fly Ash, kg | 70 | 0 | 206 |
| Ground Granulated Blast Furnace Slag, kg | 0 | 220 | 0 |
| Silica Fume, kg | 0 | 0 | 0 |
| Fine Aggregate, kg | 751 | 870 | 702 |
| Coarse Aggregate, kg | 789 | 825 | 871 |
| HRWR, kg | 9.0 | 4.4 | 10.6 |
| VMA, kg | 0 | 4.1 | .0875 |

Table 2.2 SCC Mixtures in Europe [23]

| Ingredient | Mixture 1 (powder) | Mixture 2 (VMA) | Mixture 3 (combination) |
|---|---|---|---|
| Water, kg | 190 | 192 | 200 |
| Portland Cement, kg | 280 | 330 | 310 |
| Fly Ash, kg | 0 | 0 | 190 |
| Ground Granulated Blast Furnace Slag, kg | 0 | 200 | 0 |
| Silica Fume, kg | 0 | 0 | 0 |
| Fine Aggregate, kg | 865 | 870 | 700 |
| Coarse Aggregate, kg | 750 | 750 | 750 |
| HRWR, kg | 4.2 | 5.3 | 6.5 |
| VMA, kg | 0 | 0 | 7.5 |

Table 2.3 SCC Mixtures in the United States [18]

| Ingredient | Mixture 1 (powder) | Mixture 2 (VMA) | Mixture 3 (combination) |
|---|---|---|---|
| Water, kg | 174 | 180 | 154 |
| Portland Cement, kg | 408 | 357 | 416 |
| Fly Ash, kg | 45 | 0 | 0 |
| Ground Granulated Blast Furnace Slag, kg | 0 | 119 | 0 |
| Silica Fume, kg | 0 | 0 | 0 |
| Fine Aggregate, kg | 1052 | 936 | 1015 |
| Coarse Aggregate, kg | 616 | 684 | 892 |
| HRWR, mL | 1602 | 2500 | 2616 |
| VMA, mL | 0 | 0 | 542 |

**2.4 Applications of SCC in the United States**

As the benefits of SCC become known within the industry, an increasing amount of states are looking to take advantage of this alternative building material. Several states and various federal organizations have conducted research in adopting SCC and primarily have compared it to conventional concrete under various applications to determine the viability of SCC as a building material.

*US Specific Self-Consolidating Concrete for Bridges* [24]

*Submitted to: Transportation Research Board*

Conventional concrete mixtures were used, designed specifically for bridge slabs in accordance with Michigan DOT. SCC mixture designs were created to be comparable to conventional mixtures and both were tested using standard procedures for several properties. Detailed figures for SCC and conventional concrete were created for compressive strength, freeze-thaw resistance, tensile strength, modulus of elasticity, creep and shrinkage. The SCC concrete showed a high early strength (5ksi at day 1, 7.5 ksi at day 7) which was double conventional concrete. Freeze-thaw resistance was examined and found to be sufficient after 640 cycles of testing. Segregation was tested by slump flow and cutting samples to visually inspect aggregate distribution. The SCC mixture showed excellent distribution of coarse aggregate without significant clustering of material. Finally, cost was evaluated between the two mixture designs. Due to the increased amount of cement material within SCC, a higher cost was determined. However, the paper explained that high material cost was offset by decreased labor cost and increased productivity.

*Evaluation of Self-Consolidating Concrete (SCC) for Use in North Dakota Transportation Projects* [25]

*Submitted to: North Dakota Department of Transportation*

This report contained similar testing and results compared to the previous publication. SCC mixtures were compared to similar conventional concrete mixtures and had identical proportions, except for the amount of admixture added. Properties tested include strength,

stiffness, permeability, shrinkage, durability and freeze-thaw resistance. The results showed that strength and stiffness in SCC was similar or improved compared to conventional concrete. Air voids were higher within the SCC mixture design and increased permeability. In addition to testing of SCC versus conventional concrete, a survey was conducted consisting of all 50 states' department of transportation and their usage of SCC. This report showed that only nine states (of those that responded) had specifications for the usage of SCC, while 29 states either were researching the use of SCC or actively using it within their projects in some form.

***Implementation of Self-Consolidating Concrete for Prestressed Concreted Girders*** [26]

*Submitted to: North Carolina Department of Transportation and Federal Highway Administration*

This report investigated the use of SCC for prestressed concrete girders in North Carolina. A bridge was actively being constructed during the time this investigation took place and was used to determine hardened concrete requirements. A set of three girders were tested, two made from SCC and one of conventional concrete as control. The SCC mixtures were designed and tested using standard procedures, including slump flow, VSI, and passing ability, among others. Hardened properties of all test girders were tested, such as compressive strength, modulus of elasticity, etc.  To test the feasibility of the SCC girders, load was applied to each member to simulate the design service load to determine load versus deformation properties.

Results from testing showed that SCC performed just as well, if not better in some aspects compared to conventional concrete. The hardened properties of the SCC were comparable to the conventional control girder, but the fresh properties were not optimal. A

different mixture design incorporating a larger amount of fines was suggested. When loaded to design service load, the SCC girders performed satisfactorily, showing no cracking and similar deformation and during unloading returned to its original provision. The finishes of the SCC mixtures were better than that of conventional concrete, but still contained small holes less than one-eighth of an inch. An improvement of SCC was the casting time; SCC girders took 20 minutes to cast as opposed to 30-45 minutes for conventional concrete. It was suggested that SCC usage be increased in order to take advantage of these benefits.

*Underwater Tremie Concrete Mixture Development – Lake Mead Intake #3 Tunnel Project*

*Proceedings of the Fifth North American Conference on the Design and Use of Self-Consolidating Concrete, 2013* [27]

This paper reviews the use of SCC, with specialized admixtures, to be used in an underwater environment, with long transportation time and delayed setting. 11,000 cubic yards of concrete was poured into a location 350 feet underwater and two miles from shore. Several requirements were also placed upon the concrete mixture, such as curing temperature and washout. After several different iterations of mixture design in the laboratory was completed, field testing occurred using a tremie system to pump concrete. However, there were complications with the tremie systems that caused a whole new mixture design to be developed. The anti-washout admixture caused the concrete to harden within the tremie pipes and the concrete hopper. Because of this, the anti-washout admixture was replaced with a VMA; this change solved the problems that previously occurred with the tremie system and could then be used for the project. This report specifically shows the need for field testing of SCC mixtures to

ensure that the mixture is sufficient for the job intended. By ignoring field conditions and relying only on laboratory testing, unforeseen problems can and will occur and need to be taken properly into consideration.

## 2.5 Effect of Powder Content on SCC
*Shrinkage*

Concrete with composed of high binder content is very much at risk of plastic shrinkage. Plastic shrinkage is the contraction of fresh concrete before and during setting, leading to the development of negative capillary pressure. The negative pressure causes the aggregates to pull towards each other resulting in the alteration of the concrete mass., hence shrinkage.

Turcry et al (2006) demonstrated the effect plastic shrinkage phenomenon on SCC. It was observed that with moderate evaporation, SCC mixtures exhibit plastic shrinkage before and after setting. However, SCC high windy conditions exhibited little or no difference as compared to test specimens fabricated with Ordinary concrete. It was reported that the occurrence of bleedwater, very dominant in ordinary concrete, is not the case for SCC because of its higher binder composition. The presence of bleedwater helps to reduce the evaporation of water from the concrete mass.

Roziere et al. (2007) correlated the relationship between the paste volume and shrinkage strain. Tests ran on fabricated specimens indicated that higher shrinkages strains were attained as the mortar content increases. Reduction in paste volume was reported to be inversely proportional with the amount of shrinkage cracks. A reduced internal stress generation due to the lower amount of the mortar resulted in less degrees of cracks.

Lange et al., (2008) reinforced the idea that SCC with higher paste volume will tend to exhibit higher shrinkage through internal drying from hydration. The outcome of this shrinkage is the development of high internal stresses leading to the development of cracks.

There are conflicting reports concerning the effect of shrinkage whereby the denser microstructure due to the finer powders did not lead to fabricated specimens undergoing a higher strains.

*Fracture*

The amount of coarse aggregate and the accompanying amount of the powder content is key to durability of the concrete in terms of fracture. Due to larger amount of the mortar phase in the hardened concrete matrix in SCC, it is expected to have little resistance tofracture propagation making it very less durable to meet the expected serviceability requirements.

Nikbin et al., (2014) reported that the amount of coarse aggregate in a concrete mixture has a substantial effect on the mechanical properties, most especially the fracture behavior. It was concluded that mixtures with more coarse aggregate volume with corresponding less mortar content have a higher fracture toughness compared with mixtures of the exact converse composition. Brittle number were also looked into and it came out that it increases greatly with increasing amount of coarse aggregate.

Beygi et al., (2014) corroborated the effect of powder volume on the fracture property of SCC. Not only does a lesser amount of powder reduces the tendencies for fracture, and hence less ductile, the size of coarse aggregate in the mixture also affect the fracture energies of the mixture. The more varied the aggregate blend is with the inclusion of a coarser aggregate content the more durable the concrete is with respect to fracture.

*Miscellaneous Effects*

Shear capacity is greatly influence by the amount of mortar phase and shapes of the coarse aggregate content. A higher powder content leads a wider mortar regime between coarse aggregate. Domone (2007) bolsters this theory by asserting that, since the coarse aggregates will be significantly distant from each other, the development of cracks in the mortar is allowed to grow further before it may be arrested by the closest aggregates in the line of shear.

The fresh properties of SCC is greatly hindered by the increase in volume of the powder contents in the mixture. Hypothetically, increasing the powder content enhances stability of the mixture. However, it has detrimental effect on the flowability and kinetic energy of the concrete mass. The more cohesive force there is in the fresh concrete mass, the less the flow rate of the mass.

# MATERIALS

The cement used in the research was the Type II/V Portland cement packaged by the American Eagle in Las Vegas, Nevada. The supplementary cementitious material employed is the Class F Fly Ash. It was obtained together with the coarse aggregate and sand from a local quarry plant in Las Vegas, Nevada. Purified portable drinking water with a pH of 7 was used for the design mixtures. Table 3.1 shows the physical properties of the cement, fly ash, coarse aggregate and sand used for the SCC mixtures.

Table 3.1 Physical Properties of Materials

| Material | Properties |
|---|---|
| Bulk Specific Gravity | |
| Portland Cement (Type II/V) | 3.15 |
| Fly Ash (Class F) | 2.33 |
| Sand | 2.77 |
| Coarse Aggregate (MSA: 0.75 in.) | 2.93 |
| Absorption, % | |
| Sand | 0.9 |
| Coarse Aggregate (MSA: 0.75 in.) | 0.65 |

The admixtures used in the mixing process were ADVA 195 and V-MAR 3. The inclusion of these superplasticizers (SP) is key to the attainment of certain properties typical of SCC. ADVA 195 is a polycarboxylate-based high-range water-reducing admixture. Its addition to the SCC mixtures is essential to ensure mixtures attain the desired fluidity and flowability, thereby reducing the demand of a higher water-cementitious ratios to arrive at the aforementioned properties. V-MAR 3 is a biopolymer based admixture injected into SCC mixture designs ensure their stability and prevent the washout of the mortar component from the

19

coarse aggregate. The result is a cohesive concrete composition with the likelihood of bleeding and the formation of mortar halos significantly eradicated. Table 3.2 shows the densities of the admixtures used in the SCC production.

Table 3.2 Densities of the Admixtures

| Admixtures | Density (Ib/gallon) |
|---|---|
| ADVA 195 | 8.80 |
| V-MAR 3 | 8.50 |

A constant water-to-cementitious ratio (w/c) of 0.4 and coarse aggregate with maximum sized aggregates of 0.75 inches were used throughout the research. The mixture designs worked on had different percentage composition of FA as SCM. The different percentage replacements were 25% and 35% of cementitious material. The only variables worked on to obtain the desired rheological properties were the percentage composition of the superplasticizer and the viscosity-modifying admixtures. For every mixture design, a low and a high slump SCC were engineered to give a range of the dosages required for successful mix. Therefore, a total of 4 mixture designs were embarked on with different mixture IDs to aid clarity.

The mixture IDs are:

SCC1-25L: Low slump self-consolidating concrete mixture design with 25% fly ash replacement

SCC1-25H: High slump self-consolidating concrete mixture design with 25% fly ash replacement

SCC1-35L: Low slump self-consolidating concrete mixture design with 35% fly ash replacement

SCC1-35H: High slump self-consolidating concrete mixture design with 35% fly ash replacement

Tables 3.3 and 3.4 show the batch weights and volumes for one cubic yard for each mixture respectively

Table 3.3 Batch Weights per Cubic Yard of Concrete

| Mixture Components | Mixture ID | | | |
| --- | --- | --- | --- | --- |
| | SCC1-25L | SCC1-25H | SCC1-35L | SCCI-35H |
| Cement, Ib/yd$^3$ | 493.5 | 493.5 | 493.5 | 493.5 |
| Fly Ash, Ib/yd$^3$ | 164.5 | 164.5 | 164.5 | 164.5 |
| Coarse Aggregate, Ib/yd$^3$ | 1636 | 1636 | 1636 | 1636 |
| Sand, Ib/yd$^3$ | 1337.3 | 1337.3 | 1337.3 | 1337.3 |
| Water, Ib/yd$^3$ | 271.8 | 268.2 | 272.7 | 270.2 |
| ADVA 195, % | 0.74 | 1.07 | 0.5 | 0.74 |
| VMAR 3, % | 0.17 | 0.74 | 0.17 | 0.57 |

Table 3.4 Batch Volumes per Cubic Yard of Concrete

| Mixture Components | Mixture ID | | | |
| --- | --- | --- | --- | --- |
| | SCC1-25L | SCC1-25H | SCC1-35L | SCCI-35H |
| Cement, ft$^3$/yd$^3$ | 2.5 | 2.5 | 2.18 | 2.18 |
| Fly Ash, ft$^3$/yd$^3$ | 1.13 | 1.13 | 1.58 | 1.58 |
| Coarse Aggregate, ft$^3$/yd$^3$ | 8.92 | 8.9 | 8.92 | 8.92 |
| Sand, ft$^3$/yd$^3$ | 9.8 | 9.8 | 9.69 | 9.69 |
| Water, ft$^3$/yd$^3$ | 4.16 | 4.1 | 4.18 | 4.14 |
| Air Content, % | 0.41 | 0.41 | 0.41 | 0.41 |

# EXPERIMENTAL SETUP

## 4.1 Testing: Fresh Properties

The constituents of the SCC mixes were added in a specific sequential order to ensure the homogeneity of the mix. Firstly, the coarse aggregate, cementitious materials and sand were poured into the concrete mixer sequentially, and allowed to mix for approximately 90 seconds. Secondly, three-quarter of the water is added, followed by the aqueous solution of SP and the last quarter of the water in 60 seconds. The superplasticizers, VMAR 3 and ADVA 195, are mixed with the remaining one-quarter amount of water. The mixer is turned off and the mixture is allowed to sit for an estimated period of 120 seconds. After that, the mixer is turned back on and mixing allowed to continue for 180 seconds. The effective mixing duration of the SCC mixture in the mixer is approximately 6 minutes.

The design mixtures were tested to ascertain their fresh properties and made sure they are acceptable according ASTM standards. The tests carried out to arrive at quantitative and qualitative assessment of their fresh properties were the slump flow test (ASTM C1611), J-Ring test (ASTM C1621), L-Box test and the Static Column Segregation test (ASTM C1610).The slump flow diameter, and the J-Ring flow diameter and the L-Box test values gave an indication of the fluidity and the passability of the mixture designs. Likewise, the Static Column Segregation test gave an insight on the stability of the mixtures by scientific computation of the aggregate distribution.

ASTM C1611 procedure A was undertaken to test the representative samples of the mixtures to acquire their flowability and kinetic energies. Procedure A involved the dampening and inverting the slump mold in way that the smaller circular opening faces downward touching the work surface and the bigger opening faces upwards. The representative concrete mixture is

poured continuously into the inverted slump mold to slightly overfill the mold. The slump mold

is then gradually lifted and the spread of the concrete is observed and noted.

Figure 4.1 illustrates the low and high slump flow for self-consolidating concrete with

25% FA replacements (SCC1-25L).



Figure 4.1 Low and High Slump Flow Diameters for SCC1-25

The J-Ring test (ASTM C1621) comprised of a metallic ring with metallic bar

protrusions evenly spaced around the perimeter. ASTM C1611 procedure A was employed

together with the metallic ring on every mixture design. Figure 4.2 is the ASTM C1621 test for

passing ability for a low slump self-consolidating concrete with 25% FA replacements (SCC1-

25L).

Figure 4.2 J-Ring Flow Diameter for SCC1-25L

Likewise, the Static Column Segregation test (ASTM C1610) was conducted on all the mixture designs. The apparatus used in determining the stability of the SCC included polyvinyl chloride mold. The mold consisted of sub-units continuously joined together as it is being filled with concrete. The mold connections are made mortar tight by the installations of clips. Concrete from the upper and lower molds are collected separately and washed on No. 4 sieve to extract the coarse aggregates. The extracted coarse aggregates are allowed to dry and then weighed to determine their respective masses. The sole parameter to determine their acceptability are the net weights of the coarse aggregates. Figure 4.3 shows the experimental setup for the ASTM C1610 segregation test for a low slump self-consolidating concrete with 25% FA replacements (SCC1-25L).

Figure 4.3 Static Column Segregation Test Setup for SCC1-25L

The L-Box test was ran to test the passing ability of the SCC. The apparatus used comprised of an L-shaped trough with metallic bars evenly spaced at the opening of the junction between the vertical and the horizontal trough. The opening is closed during filling of the vertical mold with concrete with a metallic plate. It is then removed to allow the fresh concrete mass to flow through the bars towards the end of the horizontal trough. The parameters needed to assess the acceptability of the mixture with regards to passing ability are the trough end depths/heights. Figure 4.4 shows the experimental setup for the L-Box test for SCC1-25L.



Figure 4.4 L-Box Experimental Setup for SCC1-25L

**4.2 Testing: Mechanical Properties**

      Cylindrical molds of diameters 4 inches and heights of 8 inches were used to cast

representative samples of the mixtures. For every SCC mixture design accepted based on the

quantitative and qualitative assessment of their fresh properties, SCC cylindrical molds were

created. Figure 4.5 shows some of lubricated cylindrical molds used for the specimen

fabrications.



Figure 4.5 Lubricated Cylindrical Molds for Specimen Fabrication

      These cylinders were cured in a convection tank at a constant temperature of $30^{o}$C until

they attained their testing age. 24 SCC cylinders were created for each mixture and were to be

used for compressive strength test (ASTM C109) and splitting tensile strength test at ages 7 and

28 days. The load application as per ASTM standards were 83 - 166 Ib/sec and 351 - 528Ib/sec

for splitting tensile test and compressive strength test respectively. Figure 4.6 shows the setups

for the compressive strength tests undertaken on fabricated specimens.

Figure 4.6 Experimental Setup for Compressive Strength Testing

The specimen failed at a low fracture energy when tested for their compressive strength. The crack development was gradual against the application of compressive stress. The alligator crack development is very much as a result of the enhanced composition of the concrete. FA with a lower specific gravity as compared to cement has the ability of achieving a denser matrix. Percentages of FA incorporated resulted in a more voluminous yet similar required weight.

Failure by tensile strength application featured a unilateral line of crack along the direction of applied stress. The development of the crack was gradual which was synonymous to that of the specimen that underwent compressive strength testing.  Figure 4.7 shows the setups for the splitting tensile strength tests carried on fabricated specimens.

Figure 4.7 Experimental Setup for Splitting Tensile Strength

The coarse aggregates in the concrete specimens were evenly distributed per visual inspection. This denotes the stability of the SCC mixtures. Static Column segregation test carried out on the fresh concrete mass strongly corroborate the aforementioned assertion. Figure 4.8 shows the coarse aggregate distribution in the hardened concrete mass for SCC1-25.



Figure 4.8 Coarse Aggregate Distribution for SCC1-25

Figure 4.9 shows the coarse aggregate distribution in the hardened concrete mass SCC1-35

Figure 4.9 Coarse Aggregate Distribution for SCC1-35

The static modulus of elasticity test (ASTM C469) was conducted on the specimens fabricated from each mixture design. A compressometer to take the strains readings coupled with the compressive testing step are assembled to ascertain the stress-strain relation of the fabricated specimens. Figure 4.10 shows the experimental setup for ASTM C469 testing ran on fabricated specimens.



Figure 4.10 Experimental Setup for Static Modulus of Elasticity Testing

### 4.3 Testing: Durability

Tests were conducted to ascertain the durability of the design mixtures. These tests were the rapid chloride penetration test (ASTM C1202), sulfate resistance (ASTM C1012) and surface scaling (ASTM C672).

RCPT was ran on specimens fabricated from each mixture design. The goal was to ascertain the permeability of the concrete specimens to chloride ions. The setup is an electrical connection between two embedded ends of a 4 inches circular disc sized specimen. Each end of the concrete discs is either embedded in a solution of sodium hydroxide (NaOH) or sodium chloride (NaCl). The concentration of the NaOH was 0.3 N in distilled water and whiles that of the NaCl was 3% by mass in distilled water. The permeability class of the concrete specimen is determined by the amount of current passed between the two ends of the disc. Figure 4.11 is the experimental setups for the rapid chloride permeability test carried out on specimens



Figure 4.11 Experimental Setup for RCPT

Fabricated specimens of each mixture underwent the test for sulfate resistance. Two groups of specimens were created, the control group of specimens were immersed in distilled

water whiles the other group were immersed in sodium sulfate solution of 50g/1000mL. This was an attempt to unequivocally and lucidly establish the effect deterioration of the sulfate attack. The immersion periods were 3, 7, and 14 days. The length and the weight attained at each immersion period of the specimens in the $Na_2SO_4$ solution were obtained. Figure 4.12 shows the experimental setup for the control immersion solution ($H_2O$) and the $Na_2SO_4$ solution for the sulfate resistance of the fabricated specimens.



Figure 4.12 Sulfate Attack Experimental Setup

The effect of deicing chemicals on the surface condition of the fabricated concrete specimens. The fabricated specimens underwent a moist-cure condition for 14 days and open-air cured for 14 days. The surface of the specimen is designed with a depression to hold the brine solution. The brine solution is a composition of 4g of anhydrous calcium chloride in 100mL of water. The specimens were then subjected to cooling condition by placing them in a freezing chamber for 18 hours and the left in the open-air condition for 6 hours. The freezing and open-air cycle is continued for 14 cycles and the brine pond was replenished at appropriate period by the addition of water. Figure 4.13 illustrates the fabrication of specimen molds for the salt scaling test.

Figure 4.13. Fabrication of Specimen Molds for Surface Scaling Test

# RESULTS

## 5.1 Fresh Properties

The parameters needed to assess the acceptability of the SCC mixtures were slump flow,

j-ring flow, $T_{50}$, L-box and static column segregation. The results were purely experimental.

Table 5.1 is the summary of results obtained from the aforementioned tests.

Table 5.1 Fresh Properties of the Concrete Mixtures

| | Mixture ID | | | |
|---|---|---|---|---|
| Mixture Components | SCC1-25L | SCC1-25H | SCC1-35L | SCCI-35H |
| Slump, in. | 20.8 | 24.5 | 21 | 25.5 |
| J-Ring,in. | 20.3 | 23.5 | 20.3 | 24.5 |
| $T_{50}$, secs. | 8 | 4 | 4 | 3 |
| L-Box (Blocking Ratio) | 0.17 | 0.1 | 0.33 | 0.14 |
| Static Column Segregation, % | 4.5 | 3.67 | 9.6 | 8.4 |

ASTM limits and guidelines were extensively used to assess the quality and acceptability

of each mixture. Qualitatively, all the mixtures were stable with respect to the visual stability

index numbers. All the mixtures had a VSI of 0. The passability of the mixtures were also

evaluated according to ASTM set limits. All the mixtures had blocking assessment values less

the 1, hence there were no signs of visible blocking from the mixtures. The stability of the

mixtures were also experimented and the values yielded were within ASTM set limits. Table 5.2

is a summary of the quantitative and qualitative analysis for each SCC mixture.

Table 5.2 Qualitative and Quantitative Assessment of the Concrete Mixtures

| Mixture ID | Visual Stability Index | Blocking Assessment | % Segregation<br>Max = 10% ~15% |
|---|---|---|---|
| SCC1-25L | Stable | No Visible Blocking<br>(0.5 in.) | 4.5 |
| SCC1-25H | Stable | No Visible blocking<br>(1 in.) | 3.7 |
| SCC1-35L | Stable | No Visible Blocking<br>(0.7 in.) | 9.6 |
| SCC1-35H | Stable | No Visible Blocking<br>(1 in.) | 8.4 |

## 5.2 Compressive and Tensile Strengths

7-day and 28-day compressive strength and splitting tensile strength of each SCC mixture were sought after. SCC1-25L and SCC1-25H attained the highest 7-day compressive and tensile strengths, and the highest 28-day compressive and tensile strengths respectively. Table 5.3 shows the 7-day and 28-day compressive and splitting tensile strength for each SCC mixtures.

Table 5.3 Compressive and Splitting Tensile Strength of the Mixtures

| Mixture ID | Compressive, PSI | | Tensile, PSI | |
|---|---|---|---|---|
| | 7 – Day | 28 – Day | 7 – Day | 28 – Day |
| SCC1-25L | 4,698 | 5,877 | 605 | 658 |
| SCCI-25H | 3,737 | 7,650 | 512 | 724 |
| SCCI-35L | 3,367 | 5,699 | 439 | 677 |
| SCC1-35H | 1,787 | 4,278 | 384 | 559 |

Figure 5.1 illustrates the 7-day compressive strengths of each of the SCC mixtures.
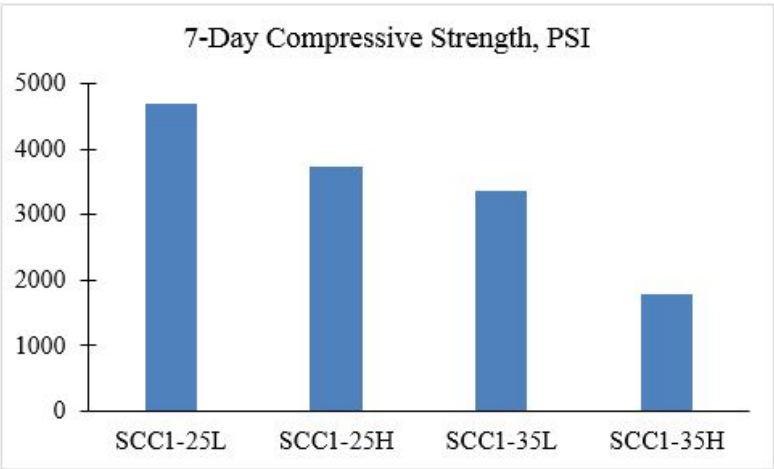


Figure 5.1 7-Day Compressive Strength of the SCC Mixtures

Figure 5.2 illustrates the 7-day splitting tensile strengths of each of the SCC mixtures.
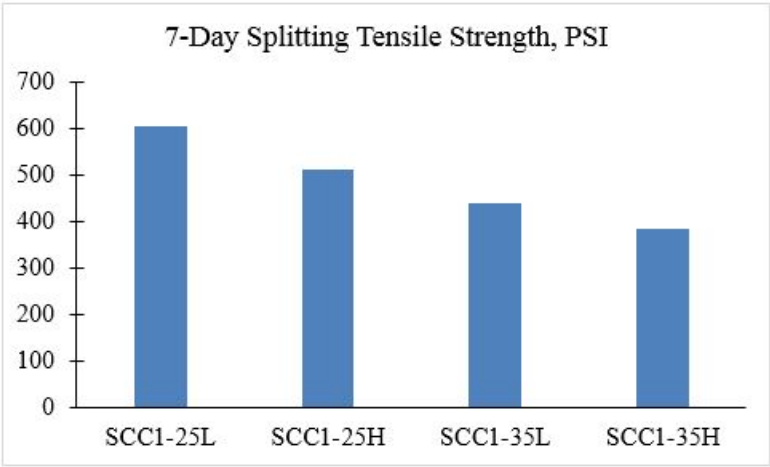


Figure 5.2 7-Day Splitting Tensile Strength of SCC Mixtures

Figures 5.3 illustrates 28-day compressive strengths of each of the SCC mixtures.
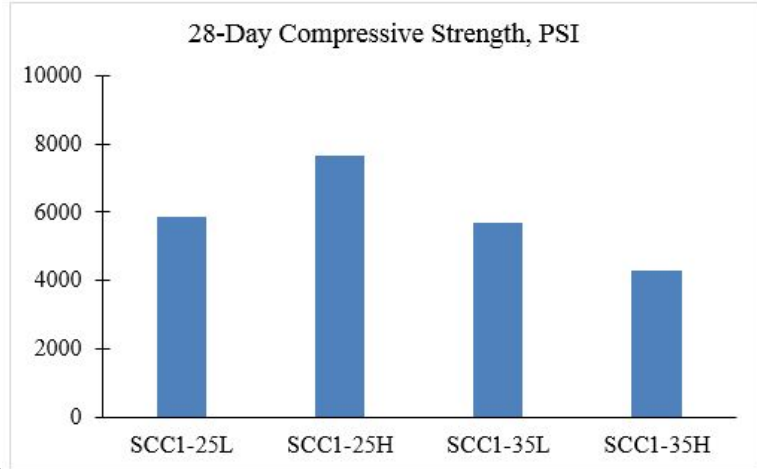


Figure 5.3 28-Day Compressive Strength of SCC Mixtures

Figure 5.4 illustrates the 28-day splitting tensile strengths of each of the SCC mixtures.
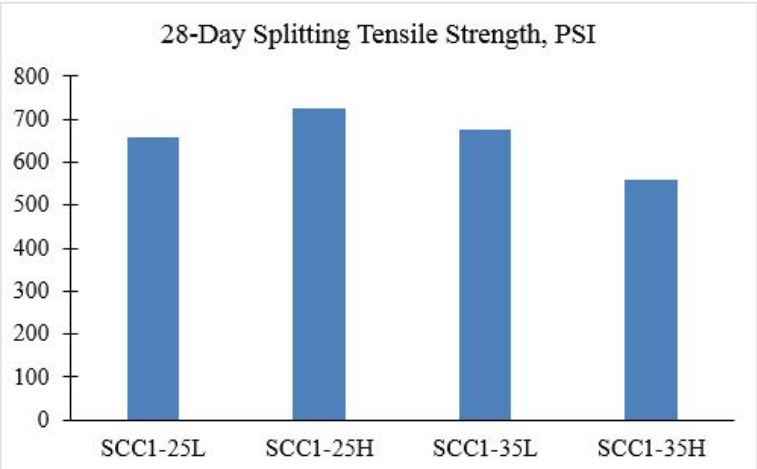


Figure 5.4 28-Day Splitting Tensile Strength of SCC Mixtures

The splitting tensile strength and the compressive strength were normalized in order to compare the ACI coefficient of 6.7 to that of the experimental coefficient. Table 5.4 shows the ACI normalized STS and that of the SCC mixtures.

Table 5.4 Normalized Splitting Tensile Strength to ACI

| | | Mixture ID | | |
|---|---|---|---|---|
| STS | SCC1-25L | SCC1-25H | SCC1-35L | SCC1-35H |
| ACI Normalized | 8.6 | 8.3 | 9 | 8.5 |
| 6.7 | | | | |

## 5.3 Modulus of Elasticity

The experimental results from the ASTM C469 were compared with values obtained from recommendations set by the American Concrete Institute. Table 5.5 shows the modulus of elasticity from the ASTM and ACI procedures.

Table 5.5 Static Modulus of Elasticity

| | SCC1-25L | SCC1-25H | SCC1-35L | SCC1-35H |
|---|---|---|---|---|
| $E=33W_c^{1.5}\sqrt{f_c}$ | 4,417,160 | 5,039,600 | 4,349,760 | 3,768,660 |
| ASTM C469 | 924,320 | 1,000,000 | 777,373 | 880,545 |

The compressive stress and strain curves were ascertained for each SCC mixture. Figure 5.5 illustrates the stress-strain curve for SCC1-25.
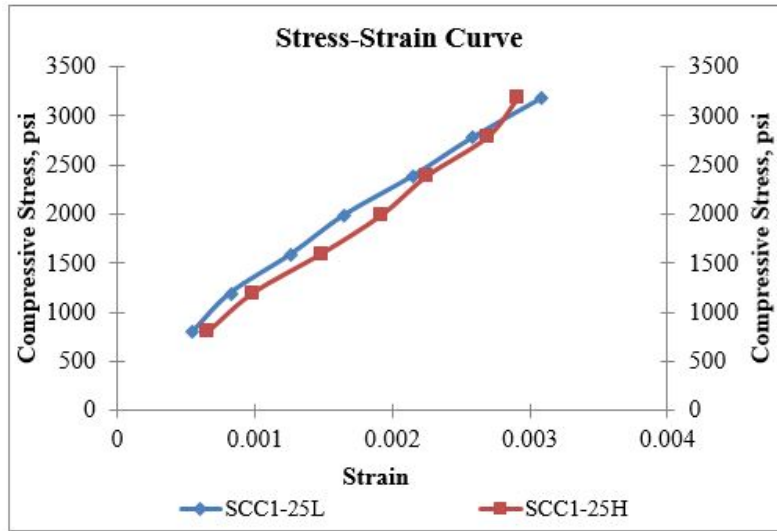
Figure 5.5 Stress-Strain Curves for SCC1-25

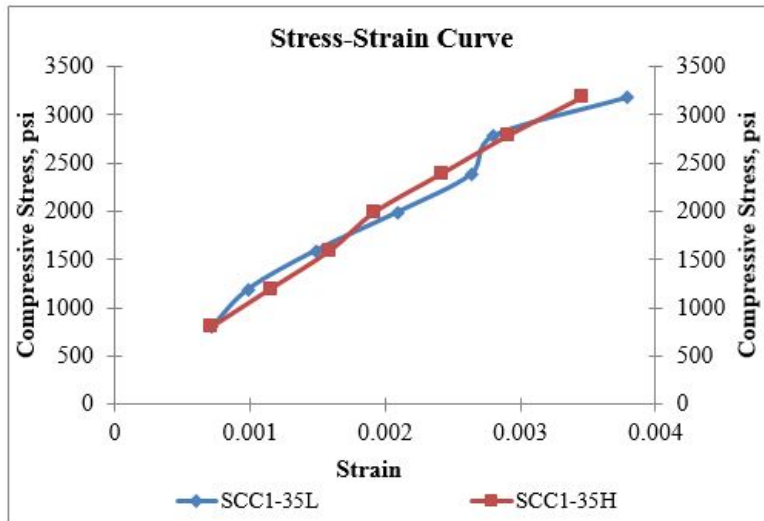Figure 5.6 illustrates the stress-strain curve for SCC1-35.



Figure 5.6 Stress-Strain Curve for SCC1-35

## 5.4 Rapid Chloride Permeability Test

RCPT test ran on the SCC specimens all had the amount of passing charge of less the

1200 coulombs. These values denoted a permeability class between very low and low. The

enhanced mortar matrix directly relates to such low values of charge passing. Table 5.6 shows

the amount of charge passed and their respective permeability classes.

Table 5.6 Rapid Chloride Permeability Test Values

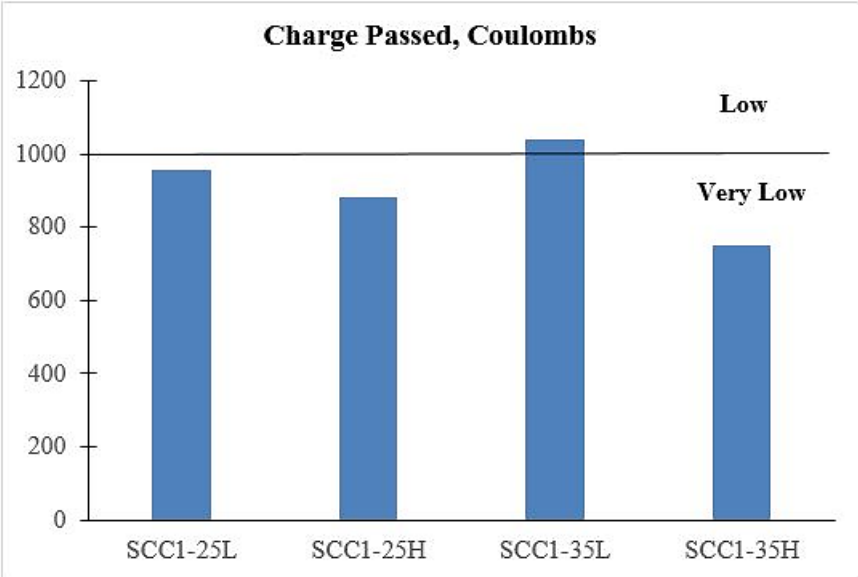| Mixture ID | Charged Passed, Coulombs | Permeability Class |
|---|---|---|
| SCC1-25L | 956 | Very Low |
| SCC1-25H | 880 | Very Low |
| SCC1-35L | 1,039 | Low |
| SCC1-35H | 751 | Very Low |



Figure 5.7 Charge Passed per SCC Mixture

**5.6 Sulfate Resistance**

The effect of sulfate attack was ascertained by measuring the weights and length changed

for specific immersions periods. Table 5.6 shows the net weights of the fabricated concrete mass

at specific immersion periods.

Table 5.7 Fabricated Concrete Mass under Sulfate Attack

| Immersion Period, week | SCC1-25L | SCC1-25H | SCC1-35L | SCC1-35H |
|:---:|:---:|:---:|:---:|:---:|
| | | Fabricated Concrete Mass, Ib | | |
| 0 | 8.6635 | 9.0575 | 8.6660 | 8.7295 |
| 1 | 8.6575 | 9.0540 | 8.6655 | 8.7290 |

Figure 5.8 shows the fabricated specimen for each SCC mixture before first ever immersion in the Na2SO4 solution.



Figure 5.8 Fabricated Specimen before Immersion

Figure 5.8 shows the fabricated specimen for each SCC mixture after 1 week of immersion in the $Na_2SO_4$ solution.

Figure 5.9 Fabricated Specimen after 1 week Immersion Period

**5.7 Salt Scaling**

The specimen were inspected a specific periods to assess the impact of the NaCl solution on the

respective depressed surfaces. The impacts of the brine solution on the surface were visually

rated with respect to ASTM C672 surface ratings.

Table 5.8 Visual ratings for surface conditions of mix design specimens

| Specimens | Surface Condition | ASTM C672 Visual Rating |
|---|---|---|
| | 5 Cycles | |
| SCC1-25L | No scaling | 0 |
| SCC1-25H | No scaling | 0 |
| SCC1-35L | Very slight scaling | 1 |
| SCC1-35H | No scaling | 0 |
| | 15 Cycles | |
| SCC1-25L | Slight to moderate scaling | 2 |
| SCC1-25H | Very slight scaling | 1 |
| SCC1-35L | Moderate scaling | 3 |
| SCC1-35H | No Scaling | 0 |

Figure 5.10 shows the fabricated specimens from each design mix after undergoing 14 days of

air-curing regime.

Figure 5.10 Specimens prior to commencement of freezing and thawing cycles

Figure 5.11 shows the specimen for both SCC1-25L and SCC1-25H after 15 cycles of freezing and thawing.



Figure 5.11 SCC1-25L (Left) and SCC1-25H (Right) after 15 freezing and thawing cycles

Figure 5.12 shows the specimen for both SCC1-35L and SCC1-35H after 15 cycles of freezing and thawing.

Figure 5.12 SCC1-35L (Left) and SCC1-35H (Right) after 15 freezing and thawing cycles

The specimen were inspected a specific periods to assess the impact of the NaCl solution on the respective depressed surfaces. The impacts of the brine solution on the surface were visually rated with respect to ASTM C672 surface ratings.

Table 5.9 Visual ratings for surface conditions of mix design specimens

| Specimens | Surface Condition | ASTM C672 Visual Rating |
|-----------|-------------------|-------------------------|
| | 5 Cycles | |
| SCC1-25L | No scaling | 0 |
| SCC1-25H | No scaling | 0 |
| SCC1-35L | Very slight scaling | 1 |
| SCC1-35H | No scaling | 0 |
| | 15 Cycles | |
| SCC1-25L | Slight to moderate scaling | 2 |
| SCC1-25H | Very slight scaling | 1 |
| SCC1-35L | Moderate scaling | 3 |
| SCC1-35H | No Scaling | 0 |

Figure 5.10 shows the fabricated specimens from each design mix after undergoing 14 days of air-curing regime.

Figure 5.13 Specimens prior to commencement of freezing and thawing cycles

Figure 5.11 shows the specimen for both SCC1-25L and SCC1-25H after 15 cycles of freezing and thawing.
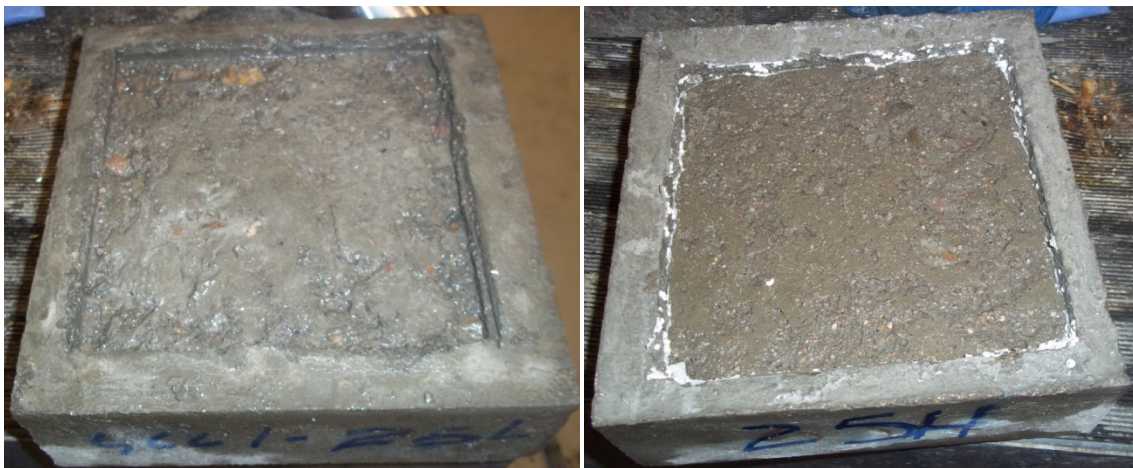


Figure 5.14 SCC1-25L (Left) and SCC1-25H (Right) after 15 freezing and thawing cycles

Figure 5.12 shows the specimen for both SCC1-35L and SCC1-35H after 15 cycles of freezing and thawing.

Figure 5.15 SCC1-35L (Left) and SCC1-35H (Right) after 15 freezing and thawing cycles

# BEHAVIOR OF CONFINED SCC

Fiber reinforced polymer (FRP) tubes have gained acceptance as an alternative to steel tubes in CFST. Precast concrete-filled fiber tubes (CFFT) offer an effective and efficient solution for accelerating construction activities (ElGawady and Sa'lan, 2011; ElGawady et al., 2010). In addition to accelerating construction, CFFT also increases the strength, ductility, and protection from corrosion of the concrete system (Lam et al., 2006). FRP tubes can be manufactured using a wet lay-up procedure or through the filament winding process. The majority of the research to date on CFFTs has been performed using FRP tubes manufactured using wet lay-up unidirectional fibers that is oriented mainly in the horizontal direction or fibers with a cross-ply (Moravvej, 2012), while very little research has been done using fibers oriented in the ±45° directions. These fibers are expected to increase the ductility of the system while still providing a moderate strength increase due to the concrete confinement.

To tailor this system for use as a precast CFFT application self-consolidating concrete (SCC) can be used to greatly increase the ease of construction and could alleviate the problem of consolidating and vibrating of the concrete under highly congested reinforcement. SCC exhibits a low resistance to flow to ensure high flowability, and a moderate viscosity to maintain a homogenous deformation through congested sections where consolidation is not practical (Khayat, 1999). SCC utilizes high dosages of superplasticizers, or high range water reducers (HRWR), and viscosity modifying agents (VMA) to increase workability while still maintaining adequate stability to suspend the aggregate at the surface of the mix.

This chapter presents the experimental results of a comprehensive investigation currently underway at the Missouri University of Science and Technology into the effects of using SCC and varying the fiber orientation for confinement under axial compression.

## 6.1 Experimental Program

A total of 28 CFFT were fabricated and subjected to axial compression loads (Table 1). The specimens were all 12 inches in height and either 6 or 6.25 in. in diameter for unconfined and confined cylinders, respectively. The specimens were examined for the following parameters:

- Fiber Orientation: FRP tubes were fabricated using ±45° bidirectional fabric , 0° unidirectional fabric , and a combination of the two

- Loading type: specimens were loaded both monotonically and cyclically

- Boundary contact: specimens were tested with either the FRP in contact with the testing machine (pre-cast application) or without (retrofit application; S). The no contact boundary was achieved by creating a precision cut 0.5 inches below the top and bottom of the tube and removing that portion of the FRP (Fig. 1).

The nomenclature of the specimens was as follows: X n YYY M-I/N-II Z where the first letter X refers to the confinement material: G for Glass FRP and C for Carbon FRP; the numeral n refers to the unconfined concrete compressive strength in ksi; the letters YYY refer to the type of concrete: SCC for standard self consolidated concrete or CC for non-flowable mixture; the numeral M refers to the fiber orientation angle: 0 for 0° or 45 for ±45°; numeral I for the number of FRP layers: I for 1 layer; the backslash "/" refers to a combination of FRP orientations with M-I being the inner FRP layers;  N-II refers to the outer FRP layers with N refers to the FRP

orientation and II refers to the number of FRP layers; is referred to as follows 45-I/0-I with the first group representing the inner layer and the second group representing the outer layers; finally, the letter Z refers to either boundary or loading conditions: S for non-contact of the FRP with the loading apparatus (Fig. 1), C for axial cyclic loading of the specimen.

### 6.1.1 Concrete

Specimens were made using both SCC and a non-flowable (conventional) concrete (CC). A SCC and CC concrete mixtures were designed and used throughout this study (Table 3). The SCC mixture was designed with a nominal max aggregate (NMS) of ¾ inch. After the SCC mixture was developed, the conventional mixture was based off this mix. To determine the effect of the flowability and possible segregation the non-flowable mixture was simply the same mix design just without the VMA and superplasticizer. A major concern with using SCC is the relatively high drying and autogenous shrinkage, especially when using low water-to-cementitious material ratios (w/cm). This could induce slipping between the concrete and FRP and reduce the overall confinement effectiveness. The fresh property tests of SCC, including slump flow, J-ring, L-box, and column segregation, were performed. Three 6 x 12 inches concrete cylinders were cast of the SCC mixture and tested in compression at 7, 28, and the day of testing, always at 56+ days after casting, to determine the compressive strength of the mixture ($\mathbf{f_c'}$). Table 4 summarizes the fresh and hardened concrete properties and figure 2 shows the unconfined concrete maximum stress of SCC and CC at different days. It was noted that the non-flowable concrete mixture experienced a late age strength gain that did not occur in the SCC mixture. This is thought to be due to the relatively high segregation of SCC. After concrete pouring, the CFFTs were allowed to harden during moist curing until the time of testing.

Table 6.1: Concrete mixture proportions

| Concrete | w/cm | Cement (lb/cy) | Fly Ash (lb/cy) | Water (lb/cy) | Fine Aggregate (lb/cy) | Coarse Aggregate (lb/cy) | HRWR (lb/cy) | VMA (lb/cy) |
|----------|------|--------|---------|-------|----------|----------|------|-----|
| SCC | 0.38 | 590 | 295 | 336 | 1,411 | 1411 | 3.6 | 1.2 |
| CC | 0.38 | 590 | 295 | 336 | 1,411 | 1411 | - | - |

Table 6.2: Fresh and hardened concrete properties

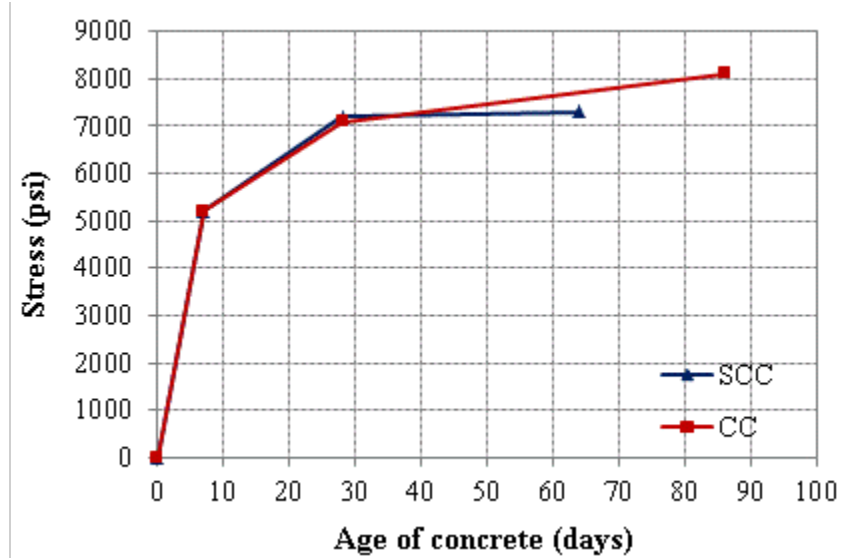| Concrete type | Slump flow/Slump (in) | J-Ring (in) | L-Box (in) | Column Segregation (%) | 7-Day Compressive Strength (psi) | $f'_c$ (psi) | $f'_{cu}$ (psi) | Age at Testing |
|---------------|----------------------|-------------|------------|------------------------|----------------------------------|--------------|-----------------|----------------|
| SCC | 27 | 25 | 0.1 | 34 | 5,200 | 7,200 | 7,300 | 64 |
| CC | 4 | - | - | - | 5,200 | 7,100 | 8,100 | 84 |

Figure 6.1: Concrete maximum stress gain

## 6.2 FRP Tubes

The tubes were fabricated using the wet layup procedure with an overlap of 5 inch. The FRP was impregnated with the epoxy and then the fabric was wrapped around a cardboard sonotube covered by aluminum foil. The excess epoxy was squeezed out of the tube, the tube was allowed to set for 24 hours before the Sono tube was removed, and the aluminum foil peeled off, producing a hollow cylindrical FRP tube. All of the tubes were air cured for at least 7 days before concrete pouring. The used CFRP and GFRP were the Tyfo® BC, SEH-51A, Tyfo® BCC, and SCH-4. All of the fibers were applied using two-component Tyfo® S epoxy. Tensile properties of the FRP were obtained from the manufacturer (Table 2).
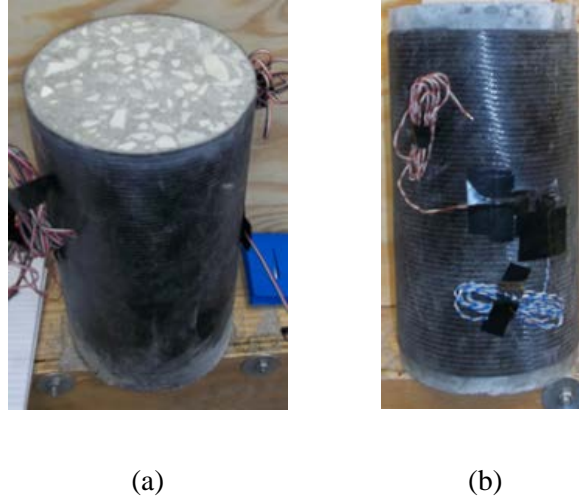
<center>(a)                        (b)</center>

Figure 6.2: (a) CFFT to be loaded as in a pre-cast application, (b) CFFT to be loaded in a retrofit

application

Table 6.3: Summary of the CFFT tested specimens data base

| Cylinder ID | $f'_{cc}$ (psi) | $\varepsilon_{cc}$ (in/in) | $\varepsilon_{cr}*$ (in/in) | $f'_{cu}$(psi) | $\varepsilon_{cu}$ (in/in) | $f'_{cc}/f'_{cu}$ | $f_r/f'_{cu}$ | $f_r$ (psi) | $\kappa_p$ | $\kappa_r*$ |
|---|---|---|---|---|---|---|---|---|---|---|
| G7SCC 45-I | 8729 | 0.0047 | 0.0145 | 7322 | 0.0026 | 1.19 | 0.06 | 440.6 | 1.78 | 5.49 |
| G7SCC 45-I S | 6736 | 0.0035 | 0.0281 | 7322 | 0.0026 | 0.92 | 0.06 | 440.6 | 1.32 | 10.65 |
| G7SCC 45-II | 9319 | 0.0035 | 0.1170 | 7322 | 0.0026 | 1.27 | 0.12 | 881.3 | 1.34 | 44.32 |
| G7SCC 45-II S | 7767 | 0.0028 | 0.0324 | 7322 | 0.0026 | 1.06 | 0.12 | 881.3 | 1.08 | 12.29 |
| G7SCC 45-III | 10122 | 0.0055 | 0.1055 | 7322 | 0.0026 | 1.38 | 0.18 | 1321.9 | 2.08 | 39.96 |
| G7SCC 45-III C | 10585 | 0.0030 | 0.0656 | 7322 | 0.0026 | 1.45 | 0.18 | 1321.9 | 1.14 | 24.86 |
| G7SCC 0-II S | 10900 | 0.0041 | 0.0094 | 7322 | 0.0026 | 1.49 | 0.38 | 2780.0 | 1.56 | 3.56 |
| C7SCC 45-I | 7764 | 0.0028 | 0.0112 | 7322 | 0.0026 | 1.06 | 0.14 | 1042.8 | 1.06 | 4.22 |

| | | | | | | | | | |
|---|---|---|---|---|---|---|---|---|---|
| C7SCC 45-I C | 8679 | 0.0032 | 0.0182 | 7322 | 0.0026 | 1.19 | 0.14 | 1042.8 | 1.21 | 6.89 |
| C7SCC 45-II | 9086 | 0.0051 | 0.1093 | 7322 | 0.0026 | 1.24 | 0.28 | 2085.7 | 1.93 | 41.40 |
| C7SCC 45-II S | 9956 | 0.0049 | 0.1128 | 7322 | 0.0026 | 1.36 | 0.28 | 2085.7 | 1.86 | 42.73 |
| C7SCC 45-III | 8549 | 0.0032 | 0.0405 | 7322 | 0.0026 | 1.17 | 0.43 | 3128.5 | 1.20 | 15.34 |
| C7SCC 45-III C | 9404 | 0.0044 | 0.0528 | 7322 | 0.0026 | 1.28 | 0.43 | 3128.5 | 1.65 | 20.02 |
| C7SCC 0-II S | 15292 | 0.0071 | 0.0893 | 7322 | 0.0026 | 2.09 | 0.52 | 3813.3 | 2.68 | 33.83 |
| G7CC 45-I/0-I | 11591 | 0.0043 | 0.0369 | 8111** | 0.0030 | 1.43 | 0.22 | 1775.0 | 1.42 | 12.31 |
| G7CC 45-I/0-I C | 11389 | 0.0088 | 0.0259 | 8111 | 0.0030 | 1.40 | 0.22 | 1775.0 | 2.94 | 8.66 |
| G7CC 45-II/0-I | 10125 | 0.0082 | 0.0378 | 8111 | 0.0030 | 1.25 | 0.27 | 2215.7 | 2.73 | 12.63 |
| G7CC 45-II/0-I C | 11454 | 0.0049 | 0.0600 | 8111 | 0.0030 | 1.41 | 0.27 | 2215.7 | 1.64 | 20.04 |
| G7CC 45-III | 9431 | 0.0036 | 0.0795 | 8111 | 0.0030 | 1.16 | 0.16 | 1321.9 | 1.19 | 26.57 |
| G7CC 45-III C | 10175 | 0.0034 | 0.0657 | 8111 | 0.0030 | 1.25 | 0.16 | 1321.9 | 1.14 | 21.94 |
| G7CC 0-II S | 11189 | 0.0041 | 0.0116 | 8111 | 0.0030 | 1.38 | 0.34 | 2780.0 | 1.38 | 3.86 |
| C7CC 45-I/0-I | 12060 | 0.0045 | 0.0661 | 8111 | 0.0030 | 1.49 | 0.35 | 2873.2 | 1.51 | 22.08 |
| C7CC 45-I/0-I C | 12201 | 0.0045 | 0.0292 | 8111 | 0.0030 | 1.50 | 0.35 | 2873.2 | 1.50 | 9.74 |
| C7CC 45-II/0-I | 12762 | 0.0084 | 0.0857 | 8111 | 0.0030 | 1.57 | 0.48 | 3916.1 | 2.80 | 28.64 |
| C7CC 45-II/0-I C | 11487 | 0.0047 | 0.1016 | 8111 | 0.0030 | 1.42 | 0.48 | 3916.1 | 1.57 | 33.94 |
| C7CC 45-III | 10196 | 0.0041 | 0.1297 | 8111 | 0.0030 | 1.26 | 0.39 | 3128.5 | 1.38 | 43.33 |
| C7CC 45-III C | 10580 | 0.0036 | 0.0910 | 8111 | 0.0030 | 1.30 | 0.39 | 3128.5 | 1.22 | 30.40 |
| C7CC 0-II S | 15593 | 0.0078 | 0.0081 | 8111 | 0.0030 | 1.92 | 0.47 | 3813.3 | 2.60 | 2.70 |

$f'_{cc}$ - maximum confined concrete compressive stress

$\varepsilon_{cc}$ - axial strain at maximum confined concrete compressive stress

$\varepsilon_{cr}$ - axial strain at FRP rupture

$f'_c$ - maximum unconfined concrete compressive stress at 28 days

$f'_{cu}$ - maximum unconfined concrete compressive stress at the day of the test

$\varepsilon_{cu}$ - axial strain at maximum unconfined compressive stress of the day of the test

$f'_{cc}/f'_{cu}$ – confinement effectiveness

$f_r$ - FRP confinement stress

$f_r/f'_{cu}$ – Normlized FRP Confinement

$\kappa_p - \varepsilon_{cc}/\varepsilon_{cu}$

$\kappa_r^* - \varepsilon_{cr}/\varepsilon_{cu}$

* Many of the ±45° CFFT did not rupture when the testing machine reached its limits and the strain when the machine reached its limit was reported.

Table 6.4: Saturated FRP properties

| Fabric | Fiber Orientation (°) | $f_t$ (psi) | $\varepsilon_{rupture}$ (%) | $E_t$ (psi*$10^6$) | Thickness/layer (in) |
|---|---|---|---|---|---|
| Tyfo BC | ±45 | 40,500 | 1.5 | 2.7 | 0.034 |
| Tyfo SEH-51A | 0 | 83,400 | 2.2 | 3.8 | 0.05 |
| Tyfo BCC | ±45 | 95,850 | 1.4 | 7.0 | 0.034 |

| Tyfo SCH-41 | 0 | 143,000 | 1.0 | 13.9 | 0.04 |
|---|---|---|---|---|---|

## 6.3 Instrumentation

Two pairs of strain gauges were placed at two locations spaced equally around the perimeter of the tube at mid-height, strains were measured in both the axial and the hoop directions (Fig. 3). The strain gauges were 0.25 inch gauge length with 120 ohm resistance. One LVDT was placed directly behind the cylinder in the center of the cylinder to measure vertical displacement. Several specimens had string potentiometers placed around there circumference to measure the circumferential strain around the specimen.



Figure 6.3: Test setup and instrumentations

## 6.4 Test protocol

The CFFT cylinders were tested using a closed loop MTS 550 kips testing machine. The test was carried out in a displacement control with a loading rate of 0.02 in/min. The specimens were subjected to either monotonic or cyclic axial load. The cyclic testing regime consisted of three cycles at the following axial displacements; 0.02", 0.05", 0.10", 0.15", 0.20", 0.40", 0.80", and 1.20". The specimen was then tested to failure.

## 6.5 Results and discussion

## 6.6 Modes of Failure

Axial compression of the ±45° CFFT created fiber local buckling, bulging, and local ruptures throughout the specimens and failed in a very slow ductile manner. The angle-ply FRP has an ability to give high ductility by the reorientation phenomenon (Au and Buyukozturk, 2005; Abdelkarim and ElGawady, 2014). Under axial loading, the angular fiber reoriented from the initial case (+45/-45) toward the hoop direction. The 0° CFFT created a very sudden failure and a complete rupture of the FRP. When combining both of the FRPs creating a ±45°/0° hybrid, a hybrid failure mode was also observed. A global rupture occurs but it occurs much more slowly than the 0° tubes. After the rupture occurs the ±45° fibers take over and the usual buckling, bulging, and rupture occurs (Fig. 4).



a)                     b)                     c)                     d)
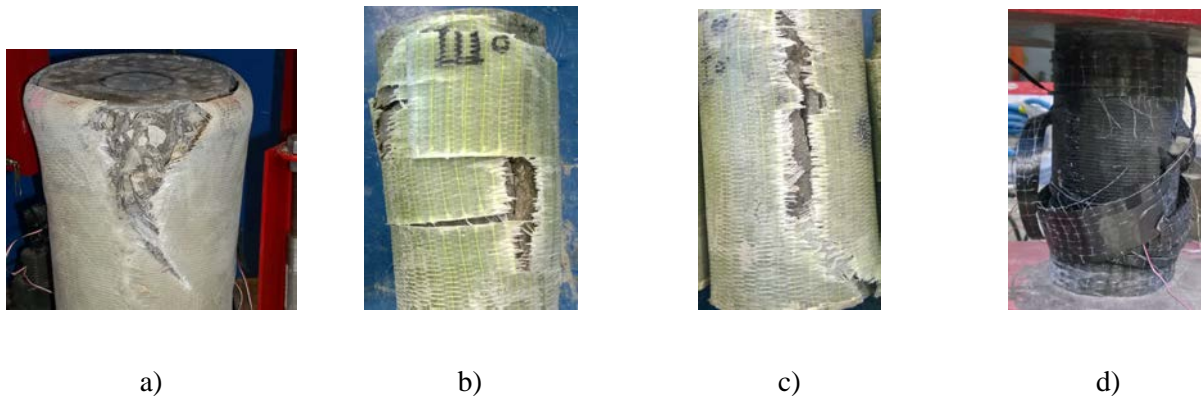
Figure 6.4. a) Rupture of a bi-directional ±45° Tube ; b) Rupture of uniaxial 0° tube ; c) Rupture of a hybrid ±45°/0° GFRP tube ; d) Rupture of a hybrid ±45°/0° CFRP tube

## 6.7 Fiber Orientation

The fiber orientation of the FRP tube has a distinct effect on not only the ultimate strength of the confined concrete but also on the ductility of the system (Fig. 5 and 6). In general, as stated in previous sections, in terms of CFFT strength the higher the confinement stress ($f_r$), the higher the confined

concrete strength. The CFFTs with unidirectional fibers, in general, have higher confinement ratio because all fibers oriented in one direction contradicting the bi-directional fibers. The fiber orientation affects the ductility and the stress-strain behavior quite significantly unlike the strength which is only slightly affected by the fiber orientation.
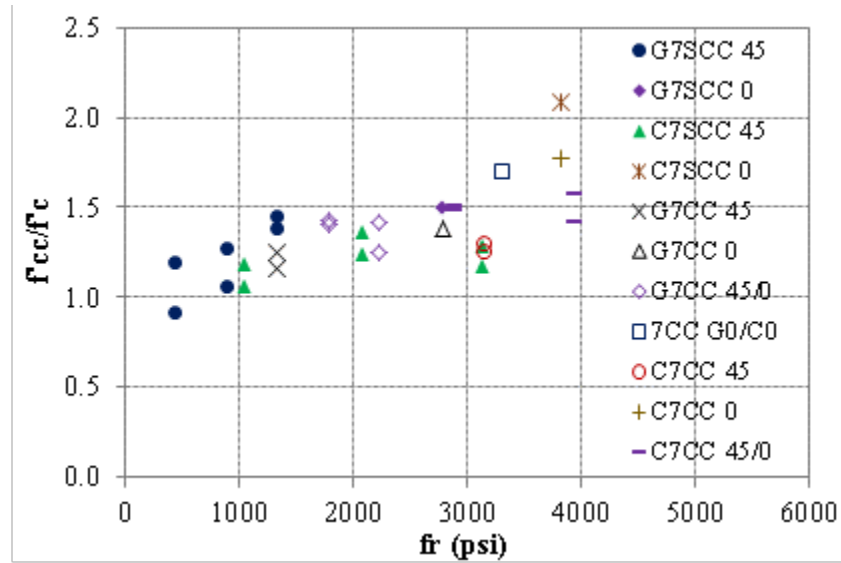


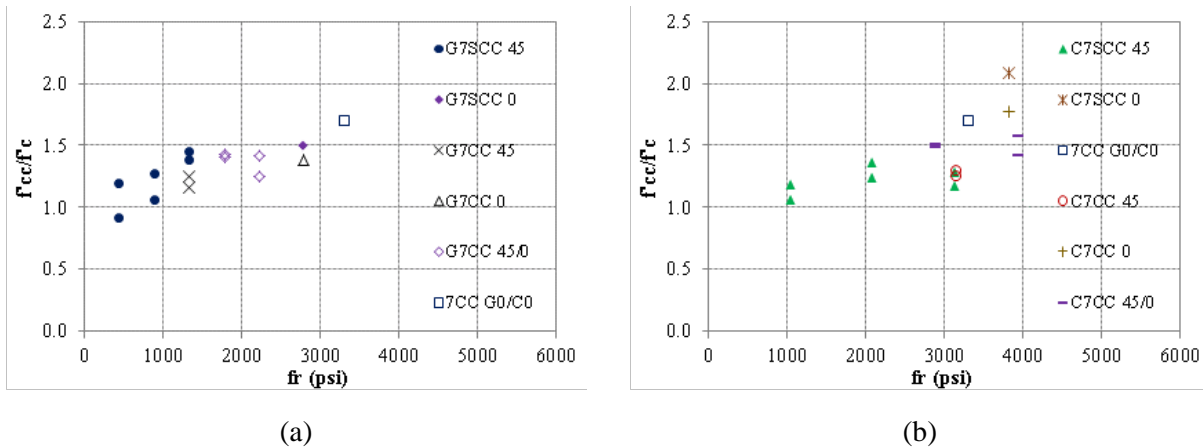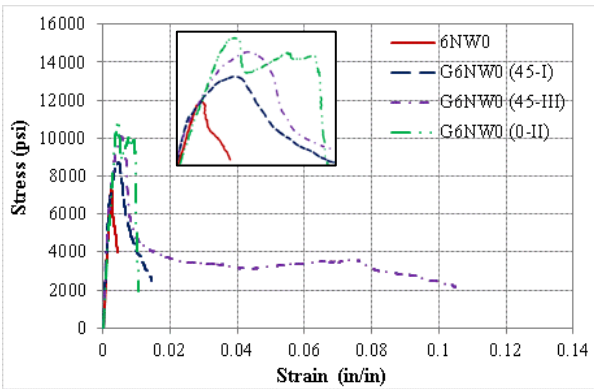Figure 6.5: Fiber Orientation effect on confinement effectiveness



(a)                                                                                          (b)

Figure 6.6: Glass and Carbon FRP effect on confinement effectiveness ; a) GFRP, b) CFRP

Though when switching Fiber orientation from the ±45° bi-directional fiber to the uniaxial 0° fiber the ductility and post peak behavior are quite different (Fig. 7). The bi-directional fibers experience a slow failure that will stabilize eventually at a residual strength and then continue on until the FRP ruptures at a very high strain. The uniaxial fibers experience a very sudden rupture of the entire FRP that occurs at much lower strains and a much lower ductility. When the mixing of the fiber orientations is present a hybrid of the two behaviors occurs. The initial behavior is much like that of the uniaxial tubes. This continues until the uniaxial fibers begin to rupture. This rupture is fairly slow in comparison to the very sudden failure experienced in the purely uniaxial tubes. Once the outer uniaxial tube ruptures the inner ±45° fiber takes over and a residual strength is obtained and maintained until the inner tube finally ruptures. These hybrid tubes were found to have a slightly lower strength than the equivalent uniaxial tube but higher than the equivalent bi-directional tube. In terms of ductility the opposite was also true, with less ductility than the bi-directional tube but more ductility than the uniaxial tube (Fig. 7).
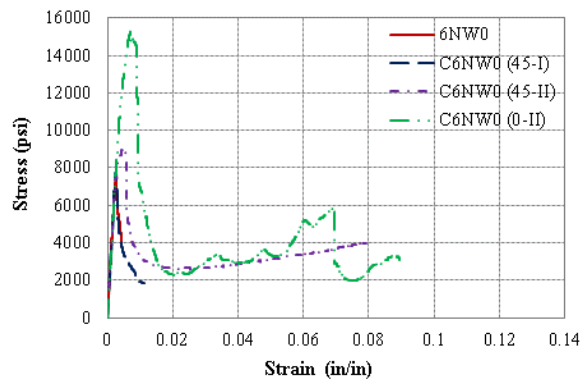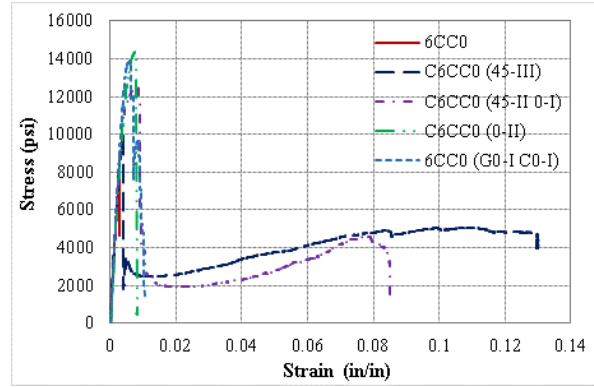


(a)                                                                (b)
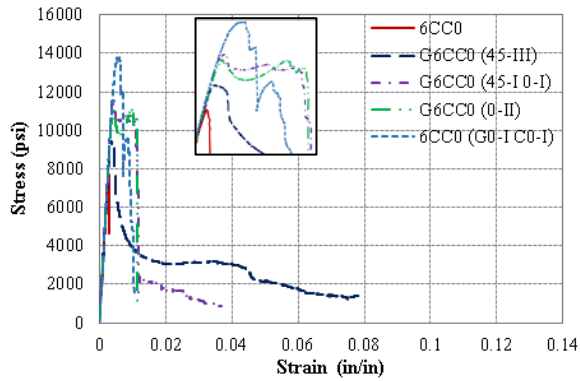
(c)                                                                            (d)

Figure 6.7:Fiber orientation effect on stress-strain behavior; a) GFRP confined SCC, b) CFRP confined

SCC, c) GFRP confined CC, d) CFRP confined CC

## 6.8 Concrete mixture effect on confinement effectiveness

SCC and its inherent issues, mainly its propensity to high shrinkage and the ever present risk of

segregation when dealing with superplasticizers, could create issues such as debonding of the FRP and

concrete creating slippage and a reduction in confinement. To determine the effect of SCC on FRP

confinement the SCC and CC mixes were compared by normalizing the strength by plotting the effective

confinement (f'cc/f'c$f'_{cc}/f'_c$) vs the confinement stress $f_r$ normalized by concrete strength ($f_r/f'_c$). (Fig. 8)

$$f_r = \frac{2t_{FRP}f_{FRP}}{D}$$

Where $t_{FRP}$ is the thickness of the FRP tube, $f_{FRP}$ is the ultimate tensile strength of the FRP tube in the

hoop direction, and D is the diameter of the concrete core.

The confinment effectivness of the non-flowable concrete, when normalized, reinforces the

trends created by the flowable concrete. This would indicate that the flowable mixture and

thenon flowable mixture can be considered the same mixture. The flowable mixture did not

experience a debonding due to the high shrinkage and using a high strength SCC mixture should

58

not present problems and could even present benefits. The normalized stress-strain curves where evaluated to see if the behavior of the flowable and non-flowable concrete where similair as well. (Fig. 9) The ±45° specimens were very similair in strength and post peak behavior. Figure 9(a) does show a difference in failure mechanism with the SCC having a much more sudden failure but the sudden release in energy didn't affect the end result, which leveled itself out over time to achieve the same residual strength. The 0° CFFT also experinced very similair behaviors indicating once again the two mixtures can be considered as one mixture. This is especially remarkable due to the segregation present in the SCC mixture. The confinement of the CFFT was not effected by the high sgregation.



(a)                                                            (b)
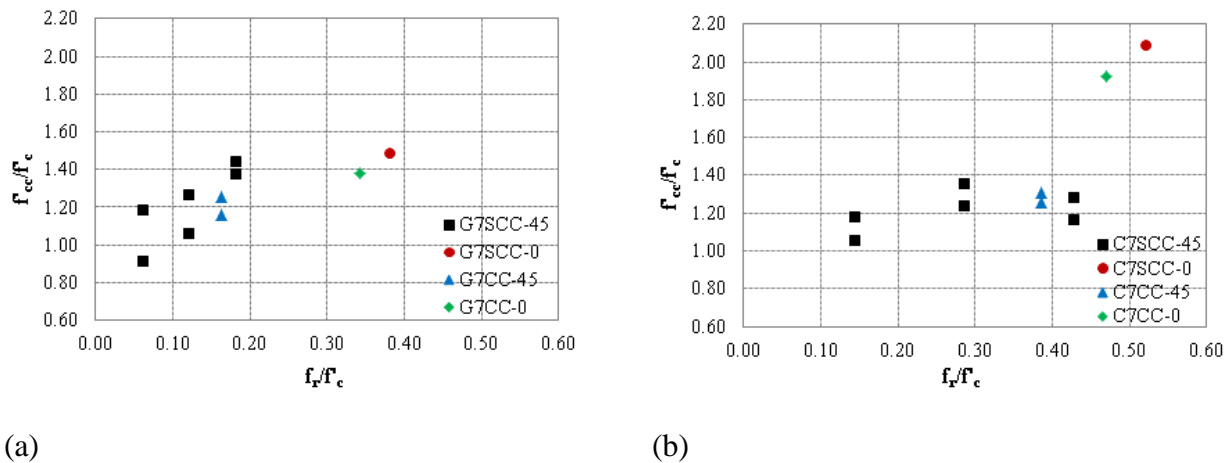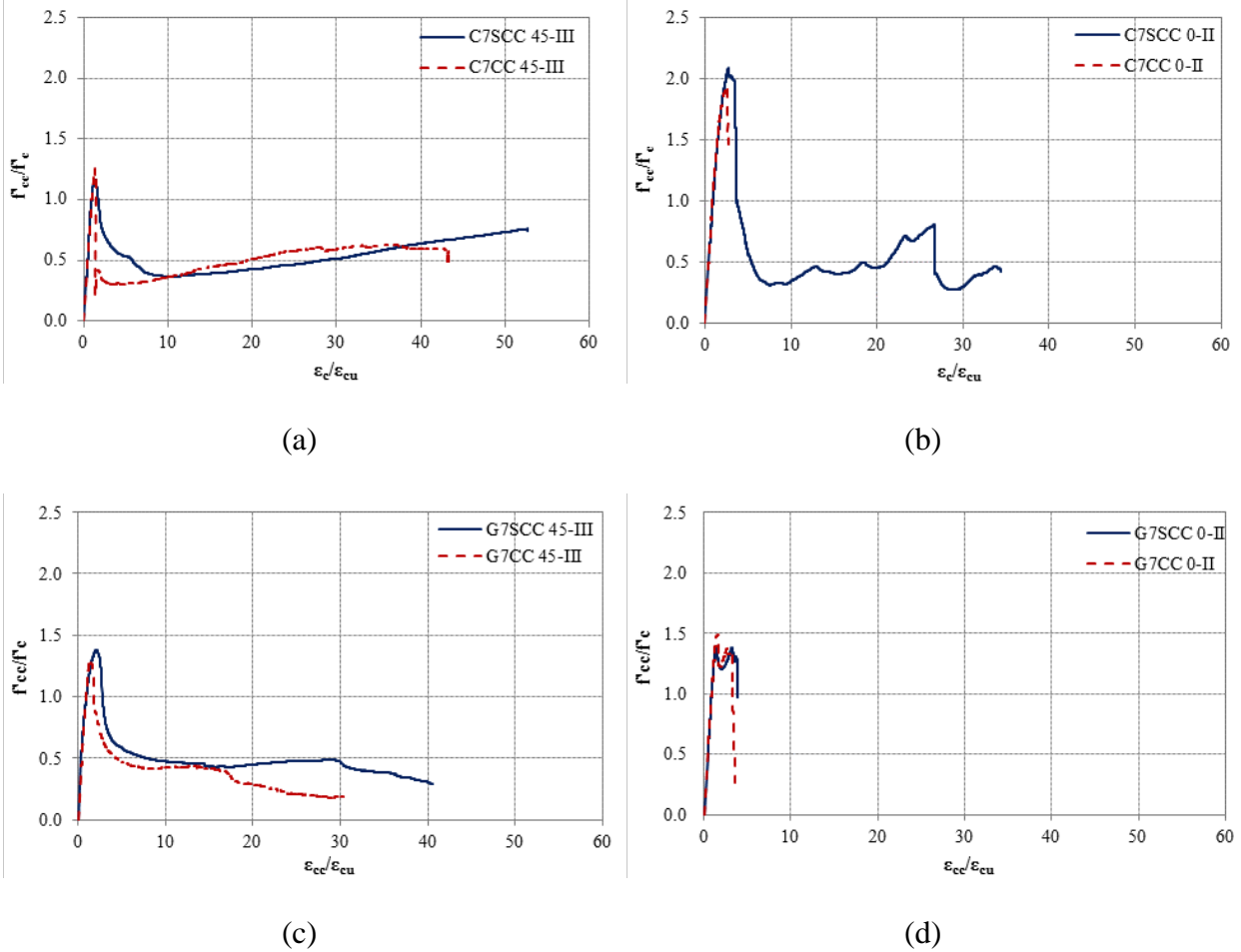
Figure 6.8: Confinement effectiveness of SCC vs CC; a) GFRP, b) CFRP

(a)



(b)



(c)



(d)

Figure 6.9: Normalized stress-strain comparison of SCC and CC; a) 3 layers carbon ±45°, b) 2 layers carbon 0°, c) 3 layers glass ±45°, d) 2 layers glass 0°

## 6.9 Fiber type effect

Both concrete filled glass FRP (GFRP) and carbon FRP (CFRP) tubes were fabricated and tested under axial compression. Although the CFRP is much stiffer than the GFRP and has a higher ultimate tensile strength this does not always corrilate to a higher confined compression strength (Fig. 10). Both Fiber types have a general trend of increasing as the stiffness increases. The ±45° CFFT did not coorelate well between the GFRP and CFRP. The GFRP has a almost linear trend

through the test while the CFRP seems to peak at 2 layers of ±45° before regressing slightly when moving up to 3 layers. In addition to this the best performing CFRP did not out perform the highest GFRP, despite having a much greater stiffness and confinement stress.

When comparing the uniaxial fiber tubes a vast difference in strength is seen, while the ductility remians very similair. The bi-directional ±45° fibers perform very differently. The ultimate strengths and coressponding strains at ultimate load are very similair. The difference between the fiber types is in the post peak behavior. After a significant drop in strength both the GFRP and the CFRP level out and stabalizes at a residual strength. This residual behavior difference between the CFRP and GFRP. The GFRP stabalizes and then slowly drops as the fiber tube ruptures down a 45° plane. The CFRP in comparison stabalizes and then experiences a slow increase. This increase has been seen to reach upwards of 60% of the original unconfined strength (Fig. 9a and 9c). The final strength at rupture could not be determined in many cases due to the limitations to the compression test setup being used. This does not seem to be the case when observing the other fiber orinetaions investigated. The 0° fibers appear to continue linearly as the confinement stress increases regardless of material. The ±45°/0° hybrid fibers also continue a similar linear trend though at a much reduced rate.


To see the differnce in behavior between the GFRP and CFRP, the specimens with the closest confinement stress to concrete strength ratio where compared (Fig. 11). The specimens followed the same general behavior though the GFRP achieves a slightly higher strength before failure, while the CFRP has a more gradual decent to its residual stress. All in all the behavior is very similair and there is little differenc in overal behavior.
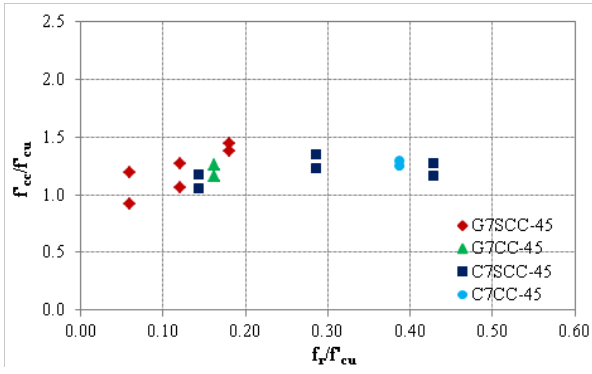
(a)
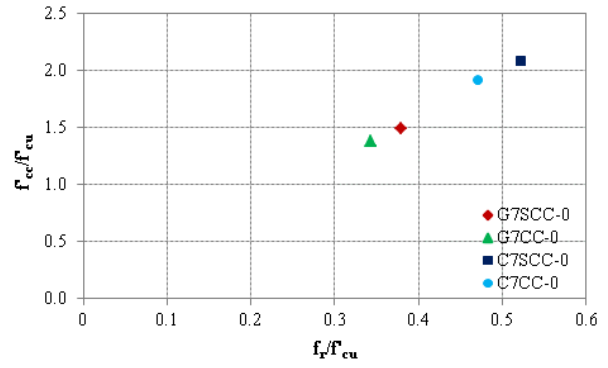
(b)
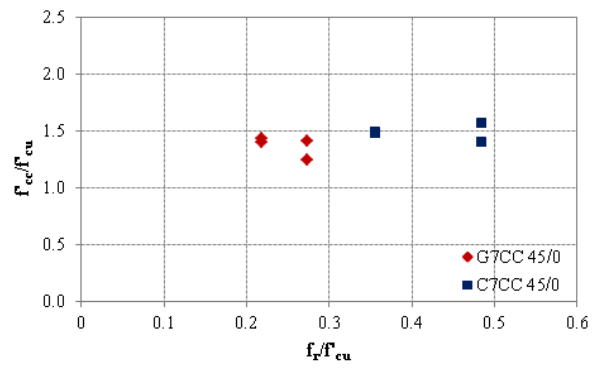
(c)

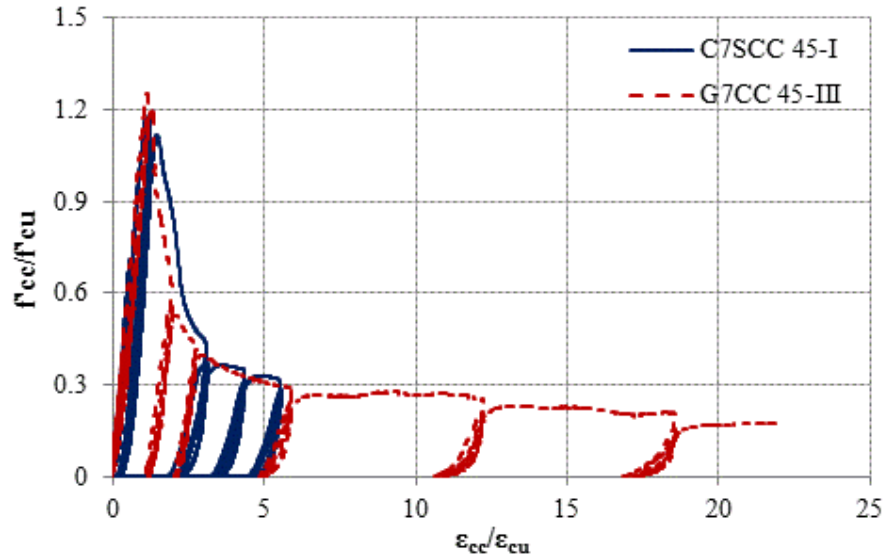Figure 6.10: GFRP and CFRP confinement effectivness; a) ±45° CFFT, b) 0° CFFT, c) ±45°/0°

CFFT

Figure 6.11: GFRP vs CFRP with similar confinement stress

## 6.10 Cyclic loading

Past research has shown that monotonic and cyclic loading produce the same stress-strain envelope (Lam et al., 2006). The FRP tubes in these cases were typically produced out of a uniaxial fiber. Tests were run to determine if this same observation also occurs when using the ±45° fibers.(Fig. 12 and 13) The cyclic loading case produced a higher load in all but one test and in most cases the increase in compression force was significant (Fig. 12). This is because the fiber reorientation toward the hoop direction is higher under cyclic loading due to the repetition of the axial load. The stress-strain behavior between the two cases is very similar though as noted above the strength is greater and the ductility is higher in the Cyclic tests (Fig.13).
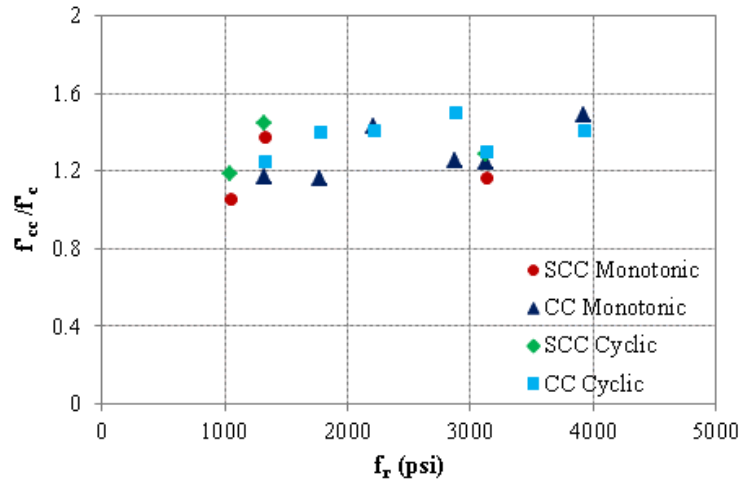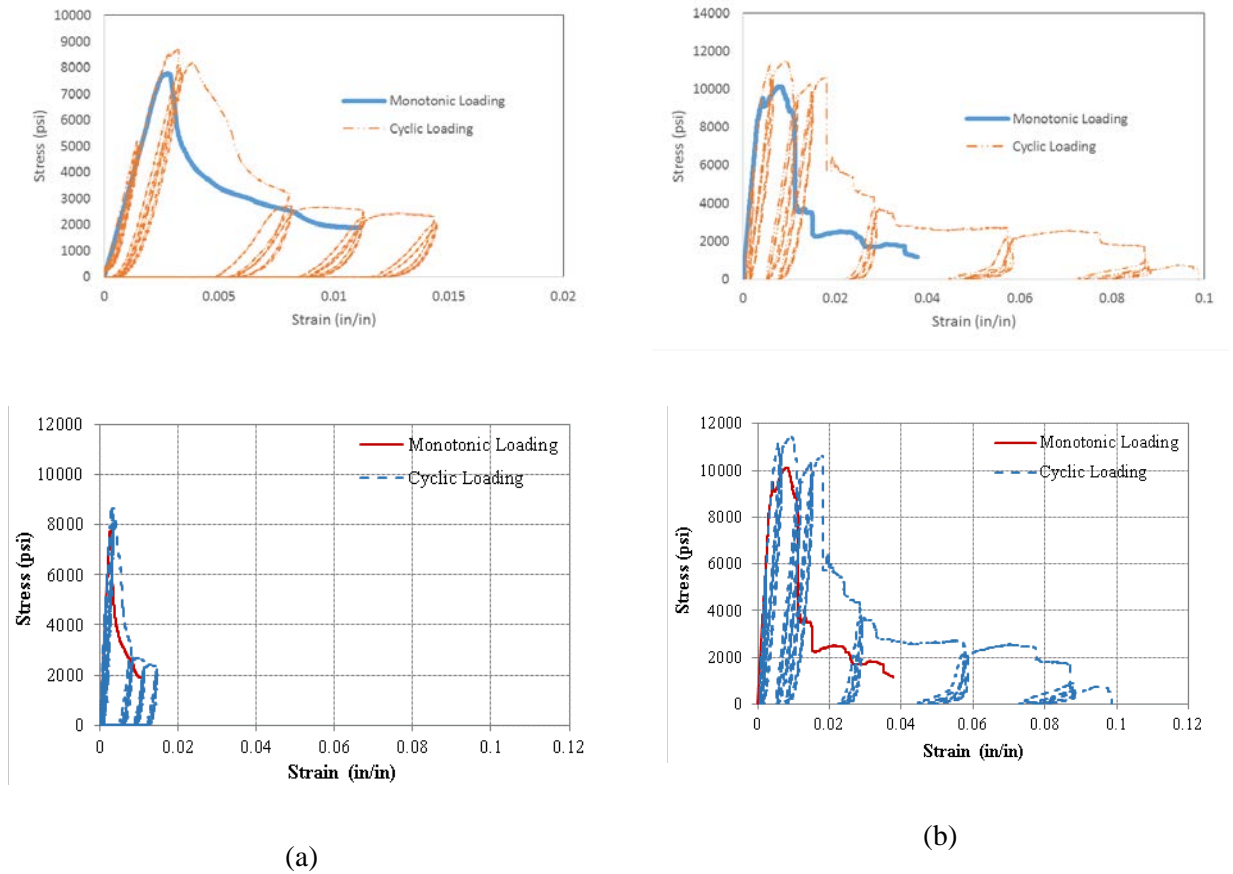
Figure 6.12: Cyclic vs Monotonic Loading



(a)

(b)

Figure 6.13: Monotonic vs cyclic stress-strain behavior; (a) Monotonic vs cyclic loading C7SCC 45-I, (b)

Monotonic vs cyclic loading G7CC 45-II/0-I

**611 Axial-lateral strain behavior**

The axial-lateral strain behavior is an indicator of the initiation of the confinement mechanisms. Figure 14(a) shows the axial-lateral strain behavior of the bi-directional GFRP tubes. The axial strains were calculated using LVDT's. The hoop strains were calculated using the string potentiometer. The behavior of the CFFT can be generalized by two bilinear sections with a small transition zone. The first zone shows the strength gaining section of the CFFT where the axial strain grows at a steady rate while the hoop strain stays about zero. This goes on until the failure of the CFFT at which time the curve shifts to the other linear portion of the curve in which the hoop strains and the axial strains grow at a steady rate. The real difference between the three is the transition zone. The one layer glass CFFT has the largest transition zone which causes the hoop strains to exceed the axial strains, while on the flip side the two and three layer transition zone are smaller and causes the axial strains and hoop strains to equal eachother and achieve a longer residual strength zone.

The carbon bi-directional CFFT axial-lateral strain behavior is shown in Figure 14(b). This shows the same general behavior as the glass but the increased stiffness of the tubes causes the transition zone to stay relatively small and the hoop strains to continue to be smaller than the axial strains. This probably explains the Carbon CFFT's propensity to have a second strength gain portion to its stress-strain curve after failure and after the residual strength has been reached and maintained.
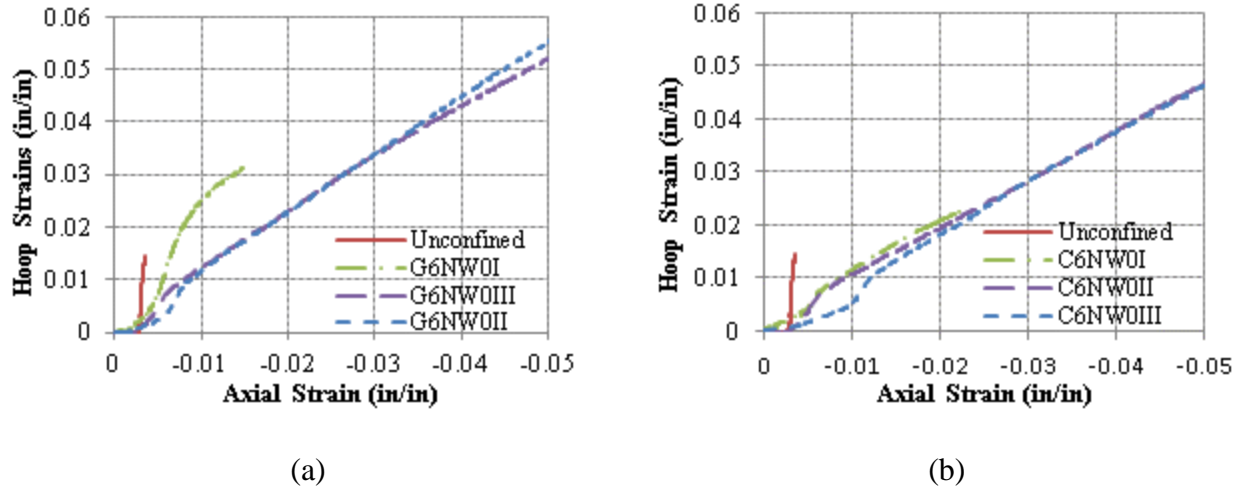
(a)                                                    (b)

Figure 6.14:. Variations of lateral strains at corresponding axial strains in (a) glass CFFT and (b)

carbon CFFT

## 6.12 Boundary Condition Effects

Specimens 1, 3, & 12 had full contact between the loading plate and the FRP tube while

specimens 2, 4, & 13 were tested by cutting strips in the FRP tube at the top and bottom. The

comparison can be seen in Figure 15. Figure 15a displays there is very little difference in stress-

strain behavior when the CFRP tube is physically loaded. Fiber reorientation comes from the

concrete lateral pressure and the axial loading pressure. As the CFRP has high stiffness, it can

attract high lateral pressure. Therefore, the general behavior did not significantly influenced by

the cutting strips. However, the ductility of the CFFT with cutting strips was higher than without

because the fiber reorientation was slower due to the concrete lateral pressure only. This is not

the case for the GFRP tube, which experienced a significant reduction in both strength and

ductility for the CFFT with cutting strips. The GFRP attracted low concrete lateral pressure

because of the low stiffness. Therefore, the fiber reorientation was significantly affected by

excluding the direct axial loading pressure on the tube. Hence, the concrete failed by crushing

and experienced very low ductility due to the low confinement with very slow fiber

reorientation.

While the stress strain relationship is the same, for the CFRP, the failure mode of the CFFT is not. The CFFT with physical loading of the FRP experienced elephant's foot local buckling of the FRP tube, where the FRP bulges at the top and the crushed concrete begins to come out. The CFFT with the strips cut in it did not experience the elephant's foot local buckling but the concrete around top and the bottom of the CFFT began to crush and spall off. Figure 16 shows both specimens during and after testing.
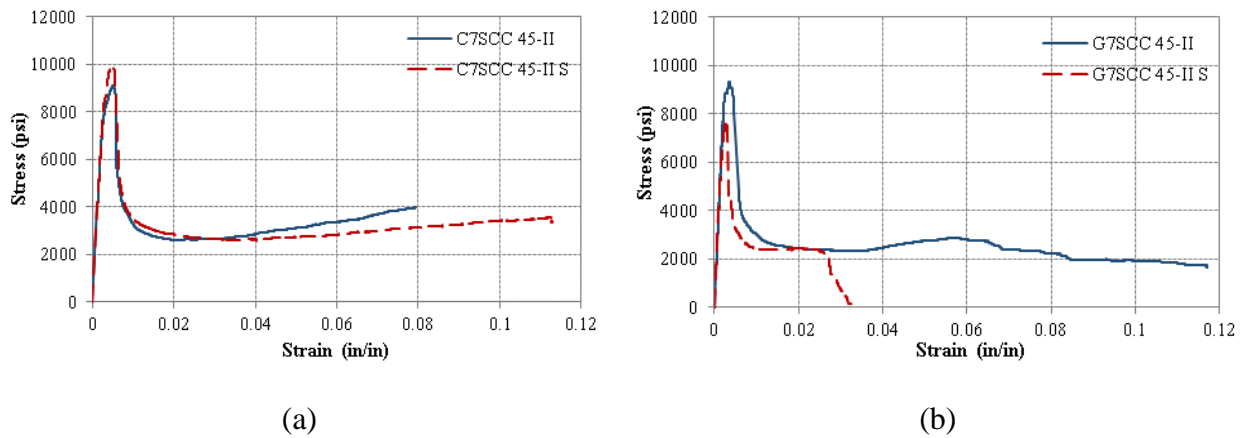


(a)                                                      (b)

Figure 6.15: Contact of the FRP tube: (a) CFRP, (b) GFRP



(a)                                    (b)                                    (c)
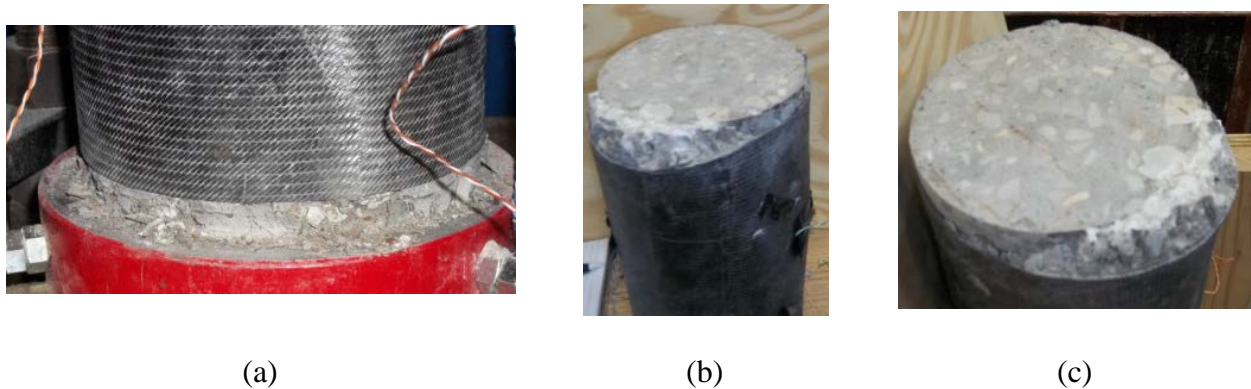
Figure 6.16: (a) Concrete crushing of specimen not in contact with the machine; (b) bulging experienced by the specimen not in contact with the machine; (c) top of specimen not in contact with the machine.

## 6.13 Comparison of Results with Existing Confinement Models

Seven existing confinement models for predicting the ultimate confined concrete strength were compared

to the experimental data collected during this investigation. The models used were proposed by Fam and

Rizkalla (2001), Harries and Kharel (2002), Marques et al. (2004), Binici (2005), Teng et al. (2007),

Samaan et al. (1998), and Sadeghian et al. (2010). These models are summarized in Table 5.

Table 6.5. FRP confined concrete models for determining f'$_{cc}$

| Proposed By: | Model |
|---|---|
| Fam and Rizkalla (2001) | $f'_{cc} = f'_c \left( 2.254 \sqrt{1 + 7.94 \frac{f_r}{f'_c}} - 2 \frac{f_r}{f'_c} - 1.254 \right)$ |
| Harries and Kharel (2002) | $f'_{cc} = f'_c + 4.269 f_r^{0.587}$ |
| Marques et al. (2004) | $f'_{cc} = f'_c + 6.7 f_r^{0.83}$ |
| Binici (2005) | $f'_{cc} = f'_c \left( \sqrt{1 + 9.9 \frac{f_r}{f'_c}} + \frac{f_r}{f'_c} \right)$ |
| Teng et al. (2007) | $f'_{cc} = f'_c + 3.5 f_r$ |
| Samaan et al. (1998) | $f'_{cc} = f'_c + 3.38 f_r^{0.7}$ |
| Sadeghian et al. (2010) | $\frac{f'_{cc}}{f'_c} = 1 + 5.18 \left( \frac{f_r}{f'_c} \right)^{0.7}$ |

The seven models were used to determine predicted confinement effectiveness and then plotted vs the

experimental confinement effectiveness determined from the experimental data collected during this

experiment. (Fig. 17 & 18) Each of the models either severely overestimated or underestimated the confinement effectiveness.
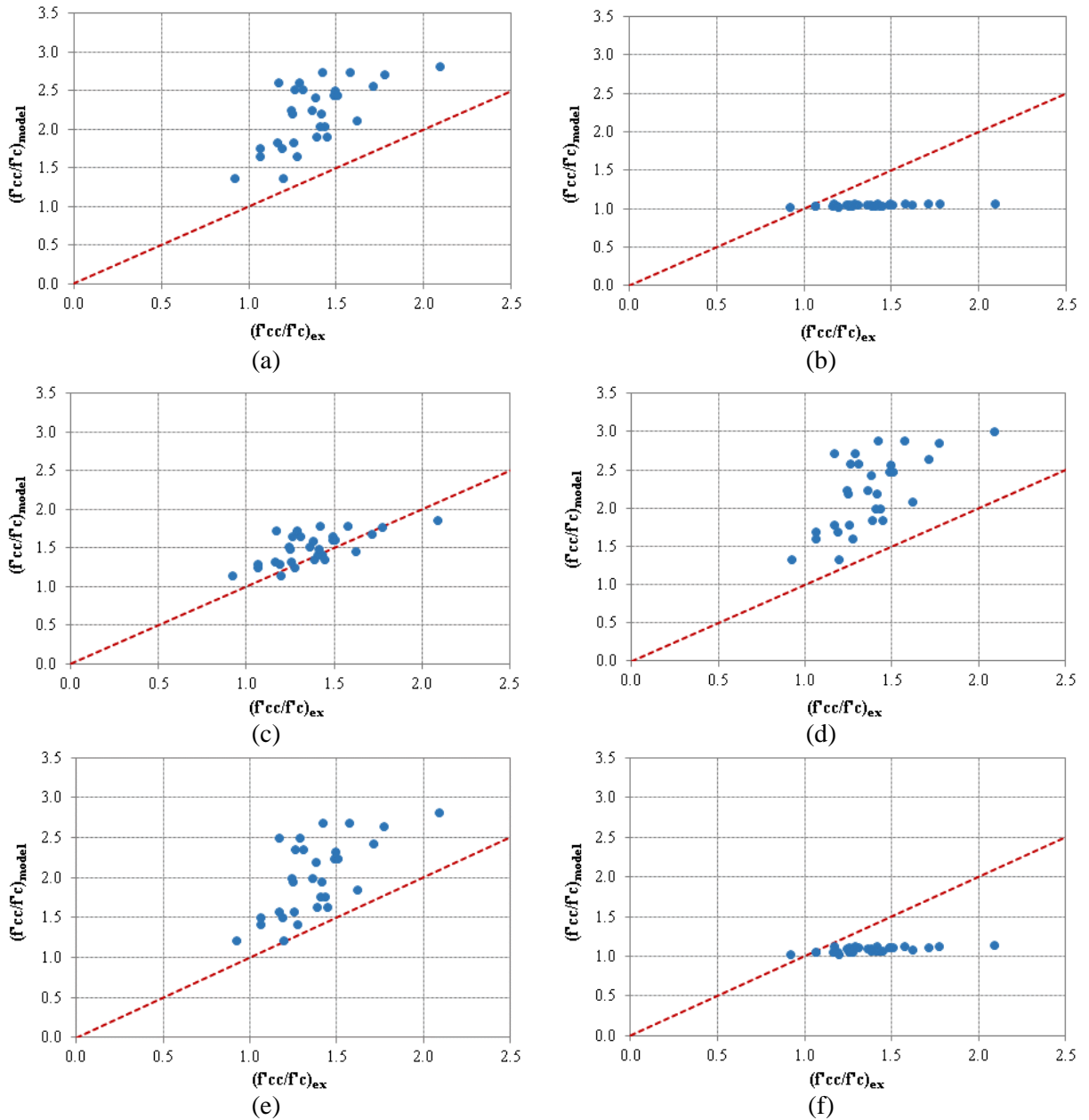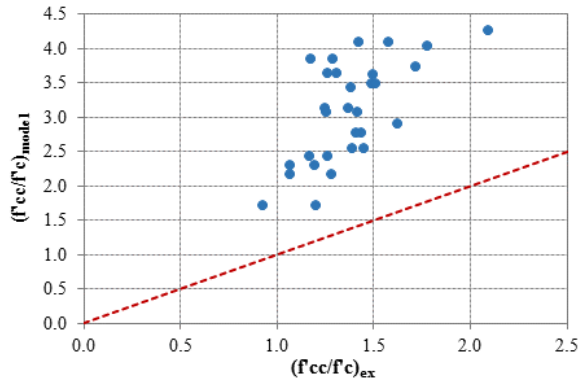


Figure 6. 17: Existing models vs experimental data; (a) Fam and Rizkalla (2001), (b) Harries and Kharel (2002), (c) Marques et al. (2004), (d) Benici (2005), (e) Teng et al. (2007), and (f) Samaan et al. (2010)

The method used to develop the seventh model was replicated to produce three proposed models for these high strength concrete cylinders (Sadeghian et al. 2010) . These models can be found in Table 6.

Table 6.6. Proposed Models for High Strength Concrete with ±45° fiber tubes

| FRP Type | Model |
|---|---|
| All Cylinders | $\dfrac{f'_{cc}}{f'_c} = 1 + 1.13 \left( \dfrac{f_r}{f'_c} \right)^{0.89}$ |
| GFRP Only | $\dfrac{f'_{cc}}{f'_c} = 1 + 1.28 \left( \dfrac{f_r}{f'_c} \right)^{0.87}$ |
| CFRP Only | $\dfrac{f'_{cc}}{f'_c} = 1 + 1.63 \left( \dfrac{f_r}{f'_c} \right)^{1.42}$ |

These models produced results much closer to the experimental values and are proposed to be used when dealing with High strength concrete confined using bi-directional fibers. These models were also plotted vs the experimental results and an additional line was added to indicated which results fall within a 10% margin of error (Fig. 6.18).
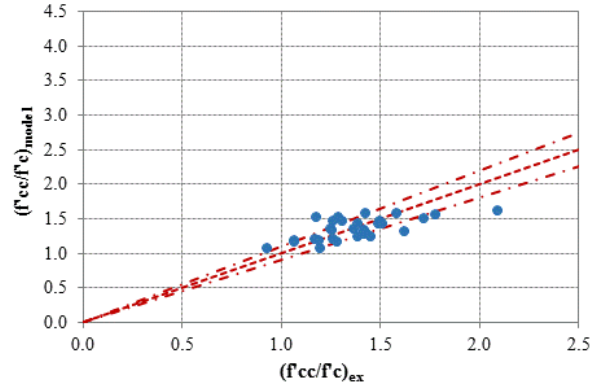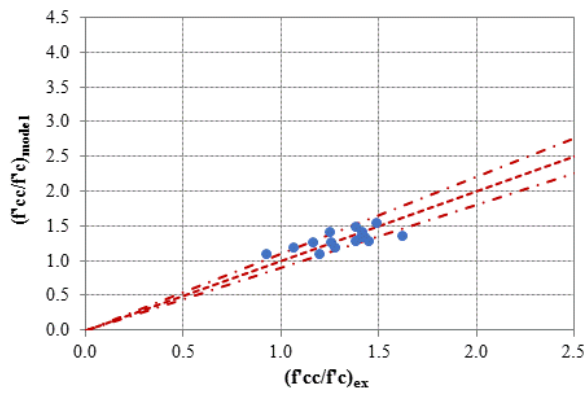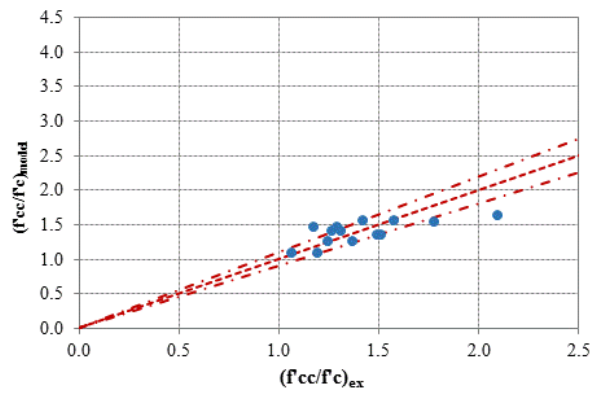
Figure 6. 18: Proposed models vs experimental data; a) Sadeghian et al., b) All cylinders, c) GFRP only, d) CFRP only

# CONCLUSIONS

The results were purely experimental and their acceptability were determined with reference to the ASTM. The following conclusions were drawn out of the experimental results and by visual inspection of the specimens.

1. The fresh properties of each SCC mixture were found acceptable with reference to ASTM. Target slump flows were closely attained as result of the inclusion of ADVA 195 and V-MAR 3. The stability of the fresh concrete mass was also enhanced by the incorporation of FA and V-MAR 3. The passing ability of the mixtures were acceptable according J-Ring test (ASTM C1621). However, L-Box tests showed that the flow and passing ability are impaired, which is predominantly as result of the level of angularity of the coarse aggregate. A rounded to a well-rounded aggregates will ensure ease of flow of the concrete mass. A maximum sized aggregate of 0.5 inches will go a long way to improve the passability of the SCC mixtures.

2. Test ran as per the static column segregation (ASTM C1610) indicated that the passing ability was acceptable. Visual inspection of the internal structures of the hardened concrete body strongly bolsters the aforementioned finding.

3. The results of the compressive strength test carried on the fabricated specimen at the age of 7 days strongly reinforces the catholic knowledge of the effect of FA on the early age compressive strength. The addition of FA to concrete mixtures retards the early age hydration of the concrete. SCC1-25 had a higher compressive and splitting tensile strength gains at the age of 7days compared to SCC1-35. The strengths are indirectly proportional to the amount replacements of FA. Likewise, the tensile strength had the same relationship with the amount of FA replacements.

4. Test values from the RCPT test indicate that the SCC mixtures were very resistant to chloride permeability. The amount of charge passed over time were all designated as either very low or low according to ASTM C1202. The inclusion of FA and the resultant enhanced microstructure has been known to contribute to the improved durability of SCC mixtures.

5. The fabricated specimens proved to be durable against sulfate attack after one week immersion in $Na_2SO_4$ solution. The mass differentials were insignificant to corroborate the high sulfate resistant ability. However, the immersion period was inadequate to finally conclude the effect of the sulfate attack.

6. The ability of the various mixtures to withstand the surface attack of deicing chemicals was assessed for 5 and 15 cycles. The surface of the specimens showed very high resistant to the brine solution after 5 cycles. However, the impact of the brine solution, even though was not extensive on most of the mixtures, was very pronounced on SCC1-35L after 15 cycles of freezing and thawing. Further mixtures and experimentation will be required to be able to really ascertain the core reason to the discrepancy on its reaction to the brine solution. In totality, the specimens had very good durability capability to deicing chemicals.

7. The use of Self-Consolidating Concrete not only meets the performance of the Conventional concrete mixture but improves the performance when the FRP tube is used as a permanent form work.  This is thought to be due to the flowability of the concrete, which allows the concrete to completely fill the tube without voids.

8. The CFRP, although stiffer, does not always produce higher strengths especially at lower confinement stresses that occur when using bi-directional ±45° fibers.

9. Cyclic loading of the tubes that use the bi-directional ±45° fiber produce higher strengths and ductility.

10. Fiber orientation has a large effect on stress-strain behavior and ductility. Bi-directional ±45° tubes experience a gradual failure that eventually reaches a residual stress before failing at relatively large strains. The uniaxial 0° fiber tubes fail very suddenly and at much lower strains. These fibers are much stiffer in the circomfrencial direction and can achieve higher strengths much more easily. When combining the two fiber types a hybrid behavior is experienced. Higher strength than the purely Bi-directional and higher ductility than the uniaxial.

# REFERENCES

1. Abdelkarim, O. I. and ElGawady, M. (2014). "Behavior of Hybrid FRP-Concrete-Steel Double-Skin Tubes Subjected to Cyclic Axial Compression." Structures Congress 2014: pp. 1002-1013.

2. ACI 237. "*Self-Consolidating Concrete*." American Concrete Institute, Farmington Hills, Michigan.

3. ACI 201. "*Guide to Durable Concrete*." American Concrete Institute. Farmington Hills, Michigan. 2008.

4. ACI 211. "*Proportioning Concrete Mixtures*." American Concrete Institute. Farmington *Hills*, Michigan. 1991. (Reapproved 2009).

5. ACI 301. "*Specifications for Structural Concrete*." American Concrete Institute. Farmington Hills, Michigan. 2010.

6. Au, C. and Buyukozturk, O. (2005). "Effect of Fiber Orientation and Ply Mix on Fiber Reinforced Polymer-Confined Concrete." J. Compos. Constr., 9(5), 397–407.

7. ASTM C1621/C1621M. "*Standard Test Method for Passing Ability of Self-Consolidating Concrete by J-Ring*." American Society of Testing and Materials. West Conshohocken, Pennsylvania. 2009.

8. ASTM C1712. "*Standard Test Method for Rapid Assessment of Static Segregation Resistance of Self-Consolidating Concrete Using Penetration Test*." American Society of Testing and Materials. West Conshohocken, Pennsylvania. 2009.

9. ASTM C1610/C1610M. "*Standard Test Method for Static Segregation of Self-Consolidating Concrete Using Column Technique*." American Society of Testing and Materials. West Conshohocken, Pennsylvania. 2010.

10. ASTM C1611/C1611M. "*Standard Test Method for Slump Flow of Self Consolidating Concrete*." American Society of Testing and Materials. West Conshohocken, Pennsylvania. 2009.

11. ASTM C143/C143M. "*Standard Test Method for Slump of Hydraulic -Cement Concrete*." American Society of Testing and Materials. West Conshohocken, Pennsylvania. 2012.

12. ASTM C1621/C1621M. "*Standard Test Method for Passing Ability of Self-Consolidating Concrete by J-Ring*." American Society of Testing and Materials. West Conshohocken, Pennsylvania. 2009.

13. ASTM C1712. "*Standard Test Method for Rapid Assessment of Static Segregation Resistance of Self-Consolidating Concrete Using Penetration Test*." American Society of Testing and Materials. West Conshohocken, Pennsylvania. 2009.

14. ASTM C1610/C1610M. "*Standard Test Method for Static Segregation of Self-Consolidating Concrete Using Column Technique*." American Society of Testing and Materials. West Conshohocken, Pennsylvania. 2010.

15. Binici, B.(2005). "An Analytical Model for Stress-Strain Behavior of Confined Concrete." Engineering Structures, 27 (7), 1040-1051.

16. Bailey, Joseph, et al. "*An Evaluation of the Use of Self-Consolidation Concrete (SCC) for Drilled Shaft Applications*." Highway Research Center and Auburn University. 2006.

17. Bernabeu and Laborde. "*SCC Production System for Civil Engineering*." Final Report of Task 8.3, Brite EuRam Contract No. BRPR-CT96-0366.

18. Beygi M.H.A.,Kazemi M.T., Amiri J.V.,Nikbin M.I., Rabbanifar S., Rahmani E. Evaluation of the Effect of Maximum Aggregate Size on Fracture Behavior of Self-compacting Concrete.*Construction and Building Materials*.Vol.55, 2014, pp. 202-211.

19. Domone P.L.Review of the hardened mechanical properties of self-compacting concrete. *Cement & Concrete Composites*. Vol. 29, 2007, pp. 1–12.

20. Dawood, H., ElGawady, M., and Hewes, J. (2012). "Behavior of Segmental Precast Post-Tensioned Bridge Piers under Lateral Loads." ASCE Journal of Bridge Engineering, Vol. 17, No. 5, pp. 735-746.

21. ElGawady, M. and Sha'lan, A. (2011). "Seismic Behavior of Self-Centering Precast Segmental Bridge Bents." J. Bridge Eng., 16(3), 328–339.

22. ElGawady, M., Booker, A., and Dawood, H. (2010). "Seismic Behavior of Posttensioned Concrete-Filled Fiber Tubes." J. Compos. Constr., 14(5), 616–628.

23. Fam, A. Z. and Rizkalla, S. H. (2001). "Confinement model for axially loaded concrete confined by circular fiber-reinforced polymer tubes." ACI Structural Journal, 98 (4), 451-461.

24. Grayson, James and Nickerson, Jim. "*Underwater Tremie Cocnrete Mix Development – Lake Mead Intake #3 Tunnel Project*." Proceedings of the Fifth North American

Conference on the Design and Use of Self-Consolidating Concrete. Chicago, Illinois. 2013.

25. Hassan E., Ahmed I., "The Properties of High-strength Self-Consolidating Concrete made with High Volume of Supplementary Cementitious Materials in Hot Weather",*5th North American Conference on the Design and Use of Self-Consolidating Concrete,* Chicago Illinois, 2013. (315)

26. Highway IDEA Project 89. "*US Specific Self Compacting Concrete for Bridges.*" IDEA Program, Transportation Research Board. Washington D.C. August 2005.

27. Hajjar J. (2000). "Concrete-filled steel tube columns under earthquake loads." Structural Engineering and Materials; 2(1):72–82.

28. Harries, K. A. and Kharel, G. (2002)."Behavior and Modeling of Concrete Subject to Variable Confining Pressure." ACI Materials Journal, 99 (2), 180-189.

29. Japan Society of Civil Engineers: Concrete Library 93. "*High-fluidity Concrete Construction Guideline.*" Japan Society of Civil Engineers. 1999.

30. Khayat, Kamal, Somnuk Tangtermsirikul. "*Fresh Concrete Properties.*" State-of-the-Art Report by RILEM Technical Committee 174-SCC. RILEM Publications S.A.R.L. 2000.

31. Koehler, Eric P. "*Use of Rheology to Specify, Design, and Manage Self-Consolidating Concrete.*" Supplementary Proceedings of the Tenth ACI International Symposium on Recent Advances in Concrete and Sustainability Issues. Sevilla, Spain. 2009.

32. Kumar P., Dubey R., "Influence of Superplasticizer Dosages on Fresh Properties of Self-Consolidating Concrete",*5th North American Conference on the Design and Use of Self-consolidating Concrete,* Chicago Illinois, 2013. (465)

33. Lam, L., Teng, J. G., Cheung, CH., and Xiao, Y.(2006) "FRP-confined concrete under axial cyclic compression." Cement & Concrete Composites, 28, 949-958.

34. Marques, SPC., Marques, DCSC., Da Silva, JL., and Cavalcante, MAA. (2004). "Model for Analysis of Short Columns of Concrete confined by Fiber-Reinforced Polymer." Journal of Composites for Construction, ASCE,, 8 (4), 332-340.

35. Lange D.A., Struble L.J, Dambrosia M.D., Shen L., Tejeda-Dominguez F., Birch B.F, Brinks A.J. Performance and Acceptance of Self-Consolidating Concrete. *Illinois Center for Transportation Series* No. 08-020 UILU-ENG-2008-2007 ISSN: 0197-9191

36. Moravvej, M., Aghahassani, M., and ElBardry, M.(2012). "The Effects of Expansive Cement on the Strength of Concrete Filled Fiber Polymer Tubes."Conference on Civil Engineering Infrastructure Based on Polymer Composites, Krakow, Poland.

37. Mamaghani, Iraj H. P., et al. "*Evaluation of Self-Consolidating Concrete (SCC) for Use in North Dakota Transportation Projects*." Department of Civil Engineering, University of North Dakota. Submitted to North Dakota Department of Transportation, Materials and Research Division. June 2008.

38. Moon, J., Lehman, D., Roeder, C., and Lee, H. (2013). "Strength of Circular Concrete-Filled Tubes with and without Internal Reinforcement under Combined Loading." J. Structural Engineering, 139(12).

39. Nikbin I.M., Beygi M.H., Kazemi M.T., J. Amiri, J.V., Rahmani E., Rabbanifar S.,Eslami M. Effect of Coarse Aggregate Volume on Fracture Behavior of Self-compacting Concrete *Construction and Building Materials.*Vol. 52, 2014, pp. 137-145.

40. Okamura, Hajime, and Masahiro Ouchi. "*Self-Compacting Concrete*." Journal of Advanced Concrete Technology. Vol. 1. 2003.

41. Phelan S. W., "Self-Consolidating Concrete (SCC): Today's Challenge and Tomorrow's Prosperity",*5$^{th}$ North American Conference on the Design and Use of Self-Consolidating Concrete,* Chicago Illinois, 2013. (281)

42. Roziere, E., S. Granger, P. Turcry, and A. Loukili. Influence of Paste Volume on Shrinkage Cracking and Fracture Properties of Self-Compacting Concrete*. Cement & Concrete Composites*. Vol. 29, No. 8, 2007, pp. 626-636.

43. RILEM Technical Committee 188-CSC: Casting of Self Compacting Concrete. "*Casting of Self Compacting Concrete*." RILEM Publications S.A.R.L. 2006.

44. Sahmaran M., Yaman I., Tokyay M. Transport and Mechanical Properties of Self-consolidating Concrete with High Volume Fly Ash. *Cement &Concrete Composites*. Vol.31, 2009, pp. 99-106.

*45.* SCC 028. "*The European Guidelines for Self-Compacting Concrete, Specification, Production and Use*." Self-Compacting Concrete European Project Group. May, 2005.

46. Su, Nan, et al. "*A simple mix design method for self-compacting concrete*." Cement and Concrete Research. Cement and Concrete Research 31. 2001.

47. Samaan, M., Mirmiran, A., and Shahawy, M. (1998). "Model of Concrete Confined by Fiber Composites." Journal of Structural Engineering, 124 (9), 1025-1031.

48. Sadeghian, P., Rahai, A.R., and Ehsani, M.R.(2010). "Effect of Fiber Orienttion on Compressive Behavior of CFRP-Confined Concrete Columns." Journal of Reinforced Plastics and Composites, 29 (9), 1335–1346.

49. Teng, J. G. Huang, Y. L., Lam, L., and Ye, L.P. (2007). "Theoretical Model for Fiber Reinforced Polymer-Confined Concrete." Journal of Composites for Construction, ASCE, 11 (2)TR-6-03. "*Interim Guidelines for the Use of Self-Consolidating Concrete in Precast/Prestressed Concrete Institute Member Plants.*" Precast/Prestressed Concrete Institute. Chicago, Illinois. April 2003.

50. Trezos  K.G., BadogiannisE.G., SfikasI.P., MakrisK.E., SmargianakiD.N.,"Properties of Self-Compacting Concrete Mixtures containing Metakaolin",5th North American Conference on the Design and Use of Self-Consolidating Concrete, Chicago Illinois, 2013. (358)

51. Turcry P., Loukili A. Evaluation of Plastic Shrinkage Cracking of Self-Consolidating Concrete. ACI Materials Journal, Vol. 4, 2006, pp. 103.

52. Wang X., Wang K., Li J., Garg N., Shah S. P., "Properties of self-Consolidating Concrete containing High Volume Supplementary Cementitious Materials and Nano-Limestone",5th North American Conference on the Design and Use of Self-Consolidating Concrete, Chicago Illinois, 2013. (415)

53. Zia, Paul, et al. "Implementation of Self-Consolidating Concrete for Prestressed Concrete Girders." Department of Civil, Construction, and Environmental Engineering, North Carolina State University. Submitted to North Carolina Department of Transportation. July 2005.